
**Title 40 CFR Part 191
Subparts B and C
Compliance Recertification Application 2019
for the
Waste Isolation Pilot Plant**

**Appendix HYDRO-2019
Hydrological Investigations**



**United States Department of Energy
Waste Isolation Pilot Plant**

**Carlsbad Field Office
Carlsbad, New Mexico**

Compliance Recertification Application 2019
Appendix HYDRO-2019

Table of Contents

HYDRO-1.0 Hydrological StudiesHYDRO-7

HYDRO-2.0 Geochemical AnalysesHYDRO-10

HYDRO-3.0 Steel-Cased Well Reconfiguration and ReplacementHYDRO-14

HYDRO-4.0 Geological InformationHYDRO-14

HYDRO-5.0 Hydraulic Test InterpretationHYDRO-15

HYDRO-6.0 Monitoring.....HYDRO-16

 HYDRO-6.1 Culebra MonitoringHYDRO-16

 HYDRO-6.1.1 Monitoring ResultsHYDRO-16

 HYDRO-6.1.2 Commercial Well PumpingHYDRO-25

 HYDRO-6.2 Magenta MonitoringHYDRO-27

 HYDRO-6.3 Dewey Lake MonitoringHYDRO-31

 HYDRO-6.4 Bell Canyon Monitoring.....HYDRO-32

 HYDRO-6.5 Monitoring SummaryHYDRO-33

HYDRO-7.0 Culebra Heads Contour Map GenerationHYDRO-34

HYDRO-8.0 Summary and Conclusions.....HYDRO-36

HYDRO-9.0 ReferencesHYDRO-36

List of Tables

Table HYDRO-1. Radiokrypton data for Culebra Dolomite groundwaters collected
2007 (Modified from Sturchio et al. 2014).....HYDRO-11

Table HYDRO-2. Wells Plugged, Abandoned, and Reconfigured, 2013—2017HYDRO-14

List of Figures

Figure HYDRO-1. Locations of WIPP Wells and Wellpads.....HYDRO-8

Figure HYDRO-2. General Stratigraphic Column of Geologic Units at the WIPP Site .HYDRO-9

Figure HYDRO-3. Detailed Rustler Formation StratigraphyHYDRO-10

Figure HYDRO-4. Histogram (solid line) of log₁₀ travel times for 55 individual realizations from the Culebra flow model boundary to well location SNL-14. Arrows indicate mode and mean of flow-model travel times, and ⁸¹Kr model age (dashed line) with counting error statistics (dotted lines) (Reproduced from Sturchio et al. 2014).HYDRO-12

Figure HYDRO-5. Map of WIPP area showing diffusion corrected ⁸¹Kr age (values in boxes, in units of 10³ years) for Culebra groundwater samples. Also shown are Rustler Formation halite margins, the Salado Formation dissolution margin, and Nash Draw (Reproduced from Sturchio 2016). .HYDRO-13

Figure HYDRO-6. Culebra Well Downhole Pressure Transducer Data CoverageHYDRO-17

Figure HYDRO-7. Water Levels in 7 Culebra Wells North of the WIPP Site.....HYDRO-18

Figure HYDRO-8. Water levels in 8 Culebra Wells in the North Portion of the WIPP SiteHYDRO-19

Figure HYDRO-9. Water Levels in 4 Culebra Wells in the North Central Portion of the WIPP Site.....HYDRO-20

Figure HYDRO-10. Water Levels in 8 Culebra Wells in the Central Portion of the WIPP Site.....HYDRO-21

Figure HYDRO-11. Water Levels in 8 Culebra Wells South of the WIPP Site.....HYDRO-22

Figure HYDRO-12. Water Levels in 6 Culebra Wells in and Near the Southeastern Arm of Nash Draw.....HYDRO-23

Figure HYDRO-13. Water Levels in Culebra Wells IMC-461 and SNL-9 West of the WIPP Site.....HYDRO-24

Figure HYDRO-14. Water Levels in Culebra Wells SNL-6 and SNL-15 East of the H2/M2 Halite MarginHYDRO-25

Figure HYDRO-15. Seven Culebra wells (H-4bR, H-9bR, H-11b4R, H-17, SNL-12, SNL-14, and SNL-17) responded visibly to short-term pumping cycles at a privately owned well. Likely pumping periods are shaded. The map insert at the lower left shows the location of the private well as a red “x” and the affected wells in the Culebra monitoring network are colored according to the plotted pressure transducer data lines (modified from Kuhlman and Corbet 2017).HYDRO-26

Figure HYDRO-16. Water Levels in 5 Magenta Wells.....HYDRO-28

Figure HYDRO-17. Water Levels in 5 Magenta Wells.....HYDRO-29

Figure HYDRO-18. Water Levels in Magenta Wells H-10a H-6c and H-8a.....HYDRO-30

Figure HYDRO-19. Magenta Well Downhole Pressure Transducer Data Coverage....HYDRO-31

Figure HYDRO-20. WQSP-6A Dewey Lake Water LevelsHYDRO-32

Figure HYDRO-21. Bell Canyon Water LevelsHYDRO-33

Figure HYDRO-22. Model-generated February 2013 freshwater head contours (10-foot contour interval) in the PA model domain. The green box indicates the area used in the WIPP ASER (DOE 2014a).HYDRO-35

Acronyms and Abbreviations

AMSL	above mean sea level
AP	analysis plan
ASER	Annual Site Environmental Report
ATTA	atom-trap trace analysis
CB	Cabin Baby
cm	centimeter
CRA	Compliance Recertification Application
DOE	U.S. Department of Energy
EPA	U.S. Environmental Protection Agency
gpm	gallons per minute
Kr	krypton
LWB	Land Withdrawal Boundary
m	meter
m ² /s	square meters per second
m ² /yr	square meters per year
min	minute
PA	performance assessment
P&A	plugging and abandonment
SNL	Sandia National Laboratories
TP	test plan
<i>T</i>	transmissivity
WIPP	Waste Isolation Pilot Plant
WQSP	Water Quality Sampling Program
yr	year

This page intentionally left blank.

HYDRO-1.0 Hydrological Studies

This appendix provides a summary of the new information on Waste Isolation Pilot Plant (WIPP) hydrology collected since January 2013 (the data cutoff for the 2014 Compliance Recertification Application [CRA-2014]), in accordance with the requirements of 40 CFR 194.15 ([U.S. EPA 1996](#)). Over that period, the U.S. Department of Energy (DOE) collected new information on the WIPP hydrogeology as a result of ongoing monitoring programs.

Section HYDRO-2.0 describes geochemical studies of radiokrypton in the groundwater of the Culebra Dolomite. Section HYDRO-3.0 lists wells replaced or plugged and abandoned since the CRA-2014. Section HYDRO-4.0 discusses geologic information collected since CRA-2014 in the WIPP monitoring network. Section HYDRO-5.0 lists hydraulic pumping and slug test analyses performed on wells in the WIPP monitoring network. Section HYDRO-6.0 describes the water-level monitoring performed since the CRA-2014, the changes in water levels that have been observed, and the effects of recent commercial pumping. Section HYDRO-7.0 discusses the generation of piezometric surface maps using the Culebra groundwater model discussed in Appendix TFIELD-2014. Section HYDRO-8.0 provides an integration of all the new hydrological information collected since the CRA-2014.

For general reference, Figure HYDRO-1 provides a map showing the locations of all wells discussed in this appendix. Figure HYDRO-2 and Figure HYDRO-3 are stratigraphic columns showing the geologic units discussed below.

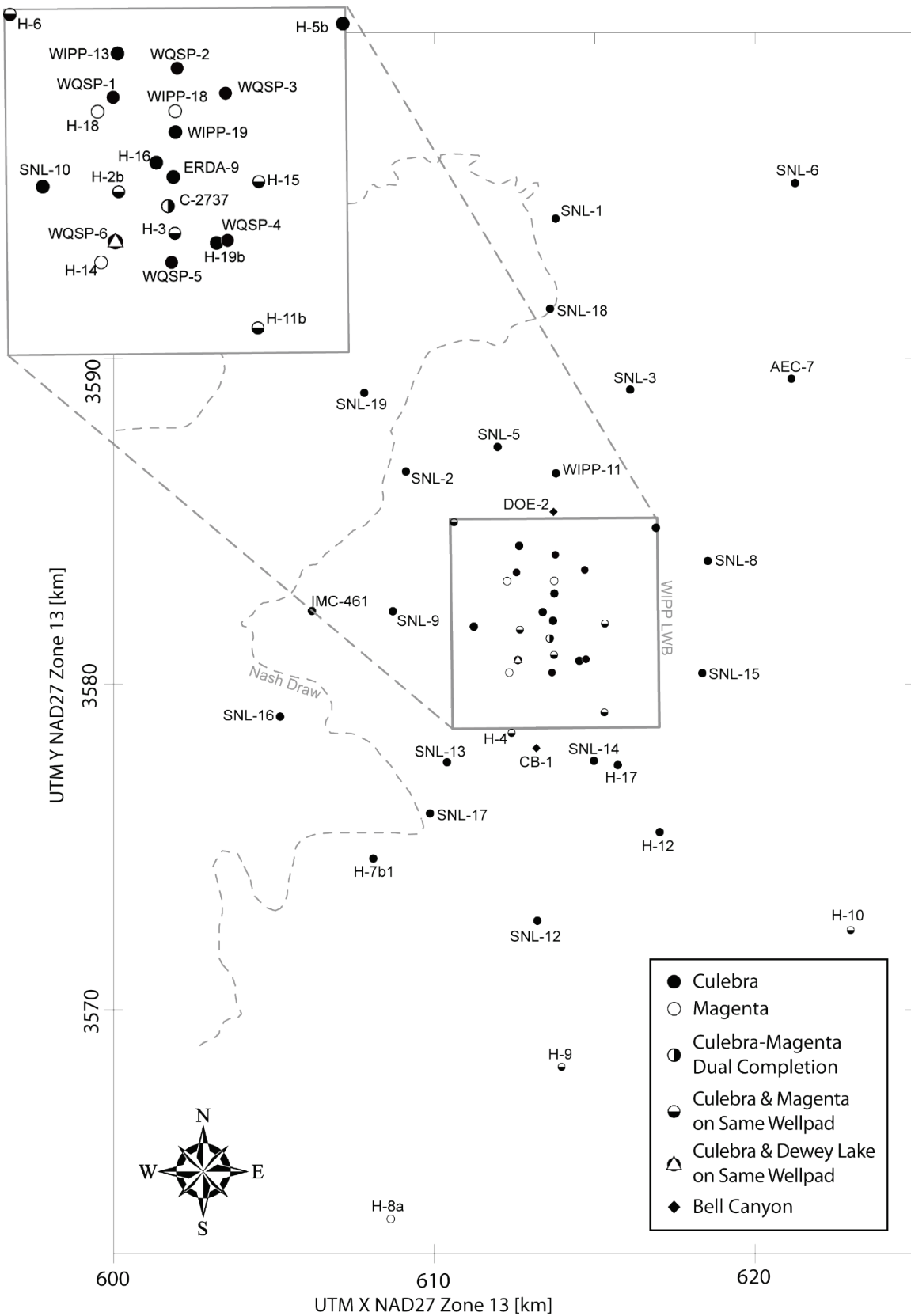


Figure HYDRO-1. Locations of WIPP Wells and Wellpads

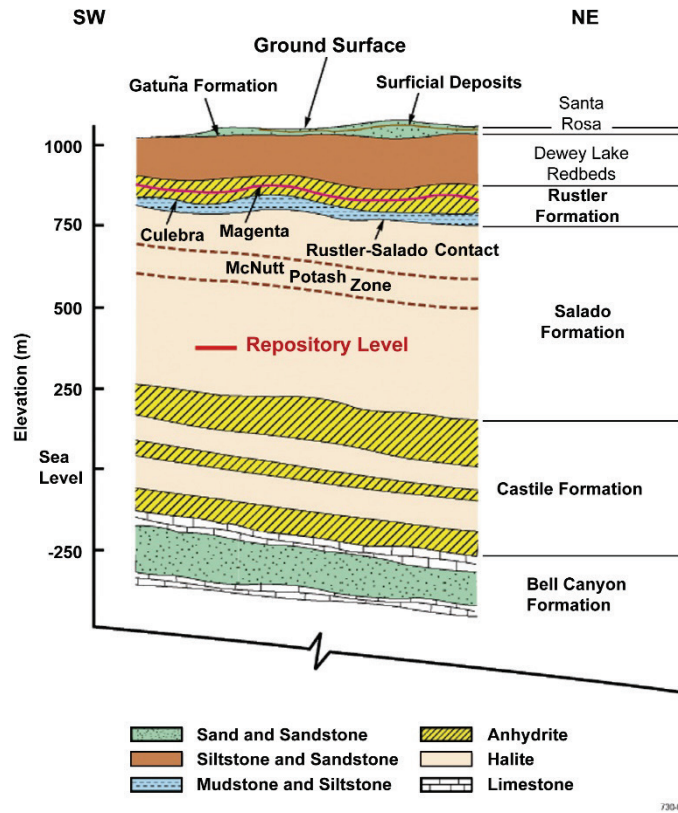


Figure HYDRO-2. General Stratigraphic Column of Geologic Units at the WIPP Site

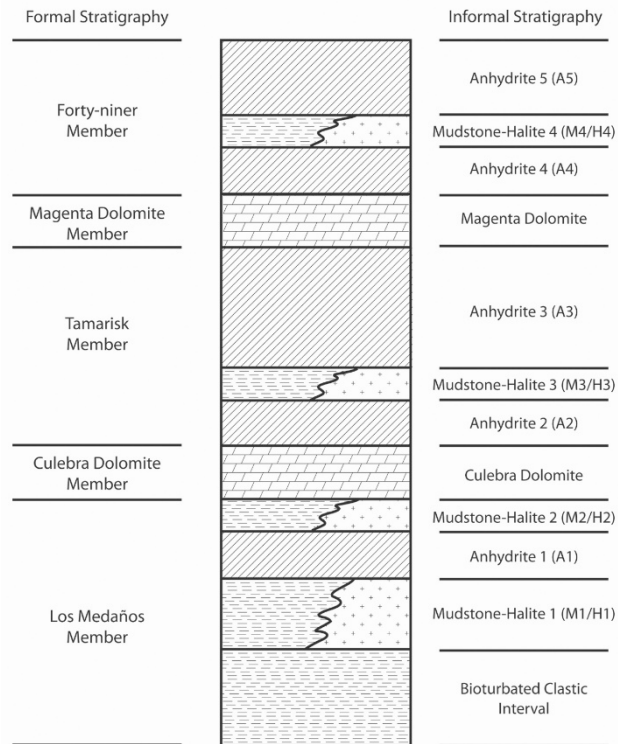


Figure HYDRO-3. Detailed Rustler Formation Stratigraphy

HYDRO-2.0 Geochemical Analyses

Two radiokrypton analyses of the groundwater were conducted in the CRA-2019 timeframe to complement the Culebra aquifer flow model and to better understand solute transport at the WIPP in accordance with Test Plan (TP) 14-01 ([Kuhlman 2014a](#)). The distribution of groundwater age at the WIPP site can give valuable information regarding transit time in the flow-regime. Data requirements for chemical isotope analysis are independent of many of the physical factors required in flow modeling. Instead, chemical isotope analysis uses concentration of radioactive or radiogenic isotopes and the rate isotopes decay or accumulate to calculate groundwater age, data which are not generally considered in groundwater flow modeling ([Bethke and Johnson 2008](#)). Combining the two approaches has the potential to refine the current understanding of transport in the Culebra aquifer.

Past attempts to utilize atmospheric tracers to evaluate the timing of recharge for Culebra groundwater have been largely unsuccessful. Chloride-36 (^{36}Cl) is not a viable tracer in the Culebra because of the saline nature of Culebra groundwater ([Phillips 2000](#)). Carbon-14 is a difficult tracer to analyze because of contamination caused by introduction of modern carbon during well drilling ([Lambert 1987](#), [Plummer and Busenburg 2008](#)). Advancements in atom-trap trace analysis (ATTA) have enabled the measurement of low-abundance radiokrypton isotopes Krypton-81 (^{81}Kr) and Krypton-85 (^{85}Kr). Krypton-81 (half-life = 229,000 years) is the best available groundwater tracer in the range of approximately 50,000 years to 1,000,000 years. Krypton-85 (half-life = 10.8 years) is somewhat more abundant than ^{81}Kr and is an ideal tracer

for young groundwater (<60 years) and/or air contamination during sampling of old groundwater (Collon et al. 2004).

Sturchio et al. (2014) presented the results of initial radiokrypton analyses using ATTA of two Culebra wells (SNL-8 and SNL-14). The wells chosen represent different transmissivity (T) zones in the Culebra Dolomite (SNL-8 $T = 10^{-6.6}$ square meters per second [m^2/s] and SNL-14 $T = 10^{-4.3} m^2/s$). Water samples from both wells have low ^{81}Kr relative to modern atmospheric air (Table HYDRO-1). Samples from SNL-8 contained measurable ^{85}Kr indicating introduction of some modern atmospheric Kr requiring correction to obtain the characteristic ^{81}Kr of the Culebra groundwater at that well site.

Table HYDRO-1. Radiokrypton data for Culebra Dolomite groundwaters collected 2007 (Modified from Sturchio et al. 2014).

Radiokrypton Data	SNL-8	SNL-14
$(^{81}Kr/Kr_{sample}) / (^{81}Kr/Kr_{atmosphere})$	0.50 ± 0.04	0.67 ± 0.05
Corrected $(^{81}Kr/Kr_{sample}) / (^{81}Kr/Kr_{atmosphere})$	0.37 ± 0.05	0.67 ± 0.05
^{85}Kr (decay $min^{-1} cm^{-3}$)	13.6 ± 1.1	<2.1

A direct comparison was made between the flow model predictions of hydraulic age and ^{81}Kr model age in well SNL-14 (Figure HYDRO-4). The ^{81}Kr model age was substantially higher than the flow model prediction of hydraulic age, which was interpreted as a constraint on the effective diffusivity of Kr in stagnant pore fluids of aquitard formations adjacent to the Culebra flow zone. Values of effective diffusivity of Kr in the stagnant zone were calculated based on the flow model predicted travel times and were constrained to 1.4×10^{-5} square meters per year [m^2/yr] to $4.7 \times 10^{-6} m^2/yr$. The low values were interpreted to imply that there is low interconnected porosity in aquitard formations and/or Kr diffusivity is slowed by adsorption or salinity effects.

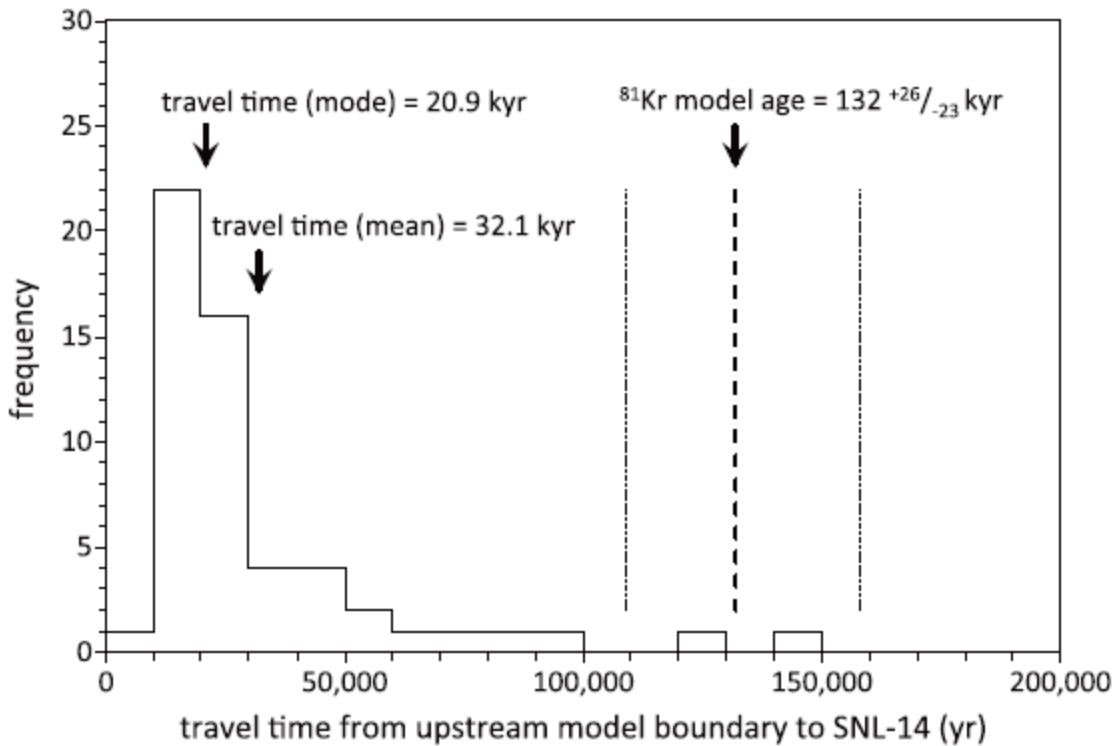


Figure HYDRO-4. Histogram (solid line) of \log_{10} travel times for 55 individual realizations from the Culebra flow model boundary to well location SNL-14. Arrows indicate mode and mean of flow-model travel times, and ^{81}Kr model age (dashed line) with counting error statistics (dotted lines) (Reproduced from [Sturchio et al. 2014](#)).

Sturchio (2016) presented the results of radiokrypton analyses of three additional Culebra wells (AEC-7R, H-12R, and SNL-16). Wells AEC-7R and H-12R are in low-transmissivity zones of the Culebra (see Section HYDRO-5.0), while SNL-16 is in a high-transmissivity zone in Nash Draw (see Figure HYDRO-1). Water samples from SNL-16 had a ^{81}Kr sample to air ratio indistinguishable from modern atmospheric Kr. Water samples from the low-transmissivity wells have low ^{81}Kr compared to modern atmosphere (0.58 sample to air ratio at AEC-7R and 0.49 sample to air ratio at H-12R), indicating long groundwater residence times of thousands of years. Sturchio (2016) used the calculation methods from Sturchio et al. (2014) to correct for the modern Kr component based on ^{85}Kr concentration and the effective diffusivity in the aquitard rock. Figure HYDRO-5 (reproduced from Sturchio 2016) shows the corrected mean residence times of Culebra groundwater at the wells sampled from both studies. The mean residence time in low-transmissivity wells SNL-14 and SNL-16 were approximately 31,000 years and <17,000 years respectively, while the residence times in low-transmissivity wells AEC-7, H-12R, and SNL-8 were approximately 48,000 years, 66,000 years, and 79,000 years respectively.

These radiokrypton studies show that ^{81}Kr measurements can be applied to saline aquifers if the effects of diffusive exchange, adsorption, and salinity gradient effects are considered. For the Culebra, we have sufficient information of the hydrogeology to apply these complicating factors to radiokrypton analyses to yield useful constraints on groundwater age and/or the effective

diffusivity of the confining units surrounding the Culebra. Radiokrypton analyses may provide a complimentary approach to far field radionuclide transport questions at the WIPP site.

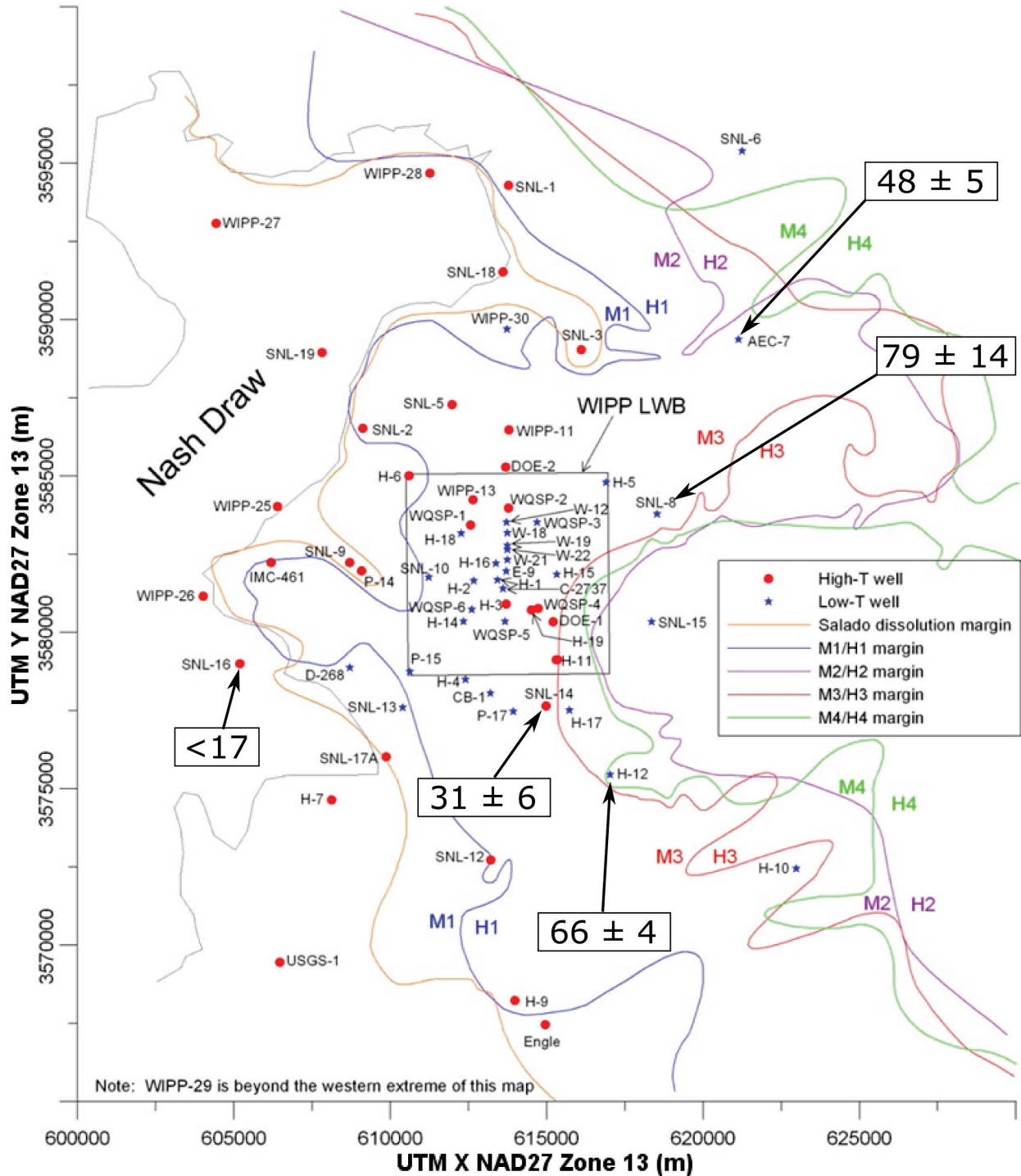


Figure HYDRO-5. Map of WIPP area showing diffusion corrected ^{81}Kr age (values in boxes, in units of 10^3 years) for Culebra groundwater samples. Also shown are Rustler Formation halite margins, the Salado Formation dissolution margin, and Nash Draw (Reproduced from [Sturchio 2016](#)).

HYDRO-3.0 Steel-Cased Well Reconfiguration and Replacement

From 1970 through 1994, all WIPP-constructed wells used steel well casing. Exposure to brine caused the steel casings to deteriorate, necessitating the plugging and abandonment (P&A) of many wells. During the peak of testing in the Culebra, many well pads had multiple Culebra wells within 50 meters (m) of one another. The cost to maintain such a density of monitoring locations is not justified based solely on the network’s use for long-term monitoring. Previously, a large number of Culebra wells located on the same well pad were plugged and abandoned. The current Culebra monitoring network is considered to have sufficient spatial coverage, and will be sustained for long-term Culebra monitoring. As the remaining steel-cased monitoring wells fail, they will be replaced with suitable fiberglass-reinforced, plastic-cased (or equivalent) wells.

Since 2013, three steel-cased wells have been plugged and abandoned (AEC-7, H-12, and H10c, see Table HYDRO-2). Three replacement wells were drilled and completed with fiberglass-reinforced plastic casings (AEC-7R, H-12R, and H-10cR). In H-series wells up to H-11 (drilled by the U.S. Geological Survey in the 1970s), a, b, and c suffixes originally referred to Magenta, Culebra, and Rustler-Salado contact completions, respectively. Well maintenance was conducted in May 2017 to repair the protective surface casing on WIPP-19 after it was damaged.

Table HYDRO-2. Wells Plugged, Abandoned, and Reconfigured, 2013—2017

Well	Interval(s) Previously Monitored	Activity	Date of Activity	Current Interval Monitored
AEC-7	Culebra	Plugged and Abandoned, Culebra Well Replaced by AEC-7R	August 2013	AEC-7R Culebra
H-12	Culebra	Plugged and Abandoned, Culebra Well Replaced by H-12R	August 2014	H-12R Culebra
H-10c	Culebra	Plugged and Abandoned, Well Replaced by H-10cR	October 2015	H-10cR Culebra
WIPP-19	Culebra	Casing Repaired	May 2017	Culebra

HYDRO-4.0 Geological Information

Between 2013 and 2017, no new monitoring well locations were drilled to obtain new geologic information of the Rustler Formation; however, replacement wells were drilled on existing well pads (Table HYDRO-2). This type of activity does not typically produce new geologic information, but cuttings and geophysical logs obtained confirm our geologic conceptual model of the Rustler Formation ([DOE 1996](#), [2016a](#) and [2016c](#)). The replacement well AEC-7R encountered a normal stratigraphic sequence for locations north-east of the WIPP site (see Figure HYDRO-1). The Culebra (the unit monitored by AEC-7R) in this location has a total thickness of 20 feet (6.1 m) and consists of vuggy textured dolomite, but also contains a large amount of gypsum ([DOE 2016a](#)). The replacement well H-12R encountered a normal stratigraphic sequence for locations south-east of the WIPP site. The Culebra in this location has a total

thickness of 27 feet (8.2 m), which also has a vuggy texture and minor amounts of gypsum present ([DOE 2016c](#)).

HYDRO-5.0 Hydraulic Test Interpretation

Hydraulic testing at the WIPP is carried out under TP 03-01 ([Schuhen 2010a](#)), while interpretation of hydraulic tests conducted at the WIPP is carried out under the Analysis Plan AP-070 ([Beauheim 2009](#)). Five analysis reports on hydraulic property parameter estimates from hydraulic tests in Culebra wells have been issued since 2013 ([Bowman 2013](#), [2015a](#), [2015b](#), [2016](#), and [2017](#)). This section only discusses hydraulic tests recently analyzed. Tests that were performed before the CRA-2014 data cut-off, but analyzed more recently are included.

Four analyses were for tests performed on Culebra replacement wells (AEC-7R, H-11bR, H-12R, and H-10cR). The results of the analyses provide estimates of Culebra transmissivity (i.e., the product of formation hydraulic conductivity and formation thickness). Bowman ([2013](#)) analyzed a constant rate pumping test conducted in June 2012 for well H-11bR. The estimated Culebra transmissivity was 2.20×10^{-5} m²/s, which compares to the average Culebra T (4.70×10^{-5} m²/s) from previous hydraulic tests on well pad H-11. Bowman ([2015a](#)) analyzed a variable rate pumping test conducted in March 2015 for well AEC-7R. The results of the analysis provided an estimate of Culebra T (6.17×10^{-7} m²/s) at AEC-7R. Bowman ([2015b](#)) analyzed a low-flow pumping test for well H-12R. The pumping test was conducted in April 2014. The estimated Culebra transmissivity was 1.53×10^{-7} m²/s at H-12R. Bowman ([2017](#)) analyzed a low-flow pumping test conducted in July 2017 for well H-10cR. The estimated transmissivity is 1.38×10^{-7} m²/s at H-10cR.

Bowman ([2016](#)) interpreted a transmissivity estimate from a suite of pneumatic hydraulic tests on well IMC-461 including sinusoidal tests, constant rate tests, and slug tests. The tests were conducted in June 2016. Analysis of the sinusoidal and constant rate tests revealed well constrained T estimates (1.78×10^{-4} m²/s and 1.36×10^{-4} respectively). Transmissivity estimates from the slug tests were not well constrained, but did have a similar value as the other test type results (9.37×10^{-4} m²/s). In addition to estimates of transmissivity, the sinusoidal tests and constant rate tests were analyzed for an estimate of storativity (2.53×10^{-4} and 4.19×10^{-4} respectively).

These data are generally consistent with past transmissivity analyses of Culebra wells in nearby areas of the monitoring network. Wells H-10cR, H-12R, and AEC-7R had low-transmissivity values similar to the wells they replaced. H-11bR and IMC-461 had higher transmissivity values in agreement with the locations of those wells (see Figure HYDRO-5 for reference to high versus low transmissivity locations).

HYDRO-6.0 Monitoring

Groundwater monitoring activities at the WIPP are carried out under the Waste Isolation Pilot Plant Groundwater Monitoring Program Plan ([NWP 2018](#)) and under Test Plan TP 06-01, Monitoring Water Levels in WIPP Wells, Revision 3 ([Schuhen 2010b](#)). The first monitoring program consists of monthly water-level measurements in all accessible wells, with results reported in the Annual Site Environmental Reports (ASERs) ([U.S. DOE 2013](#), [2014a](#), [2015](#), [2016b](#) and [2017](#)). The second monitoring program involves both periodic water-level measurements and continuous measurement (typically at 1-hour intervals) of fluid pressure in wells instrumented with downhole pressure gauges.

Water-level monitoring provides a general picture of the changes in hydraulic head occurring in the formations being monitored. Water levels are currently being monitored in the Culebra and Magenta Members of the Rustler Formation, the Dewey Lake (Redbeds) Formation, and the Bell Canyon Formation. The monitored well locations are shown in Figure HYDRO-1. Reconfigured or plugged and abandoned wells are listed in Table HYDRO-2.

HYDRO-6.1 Culebra Monitoring

HYDRO-6.1.1 Monitoring Results

In addition to monitoring Culebra water levels, DOE monitors the fluid pressure in many wells with downhole pressure transducers. The history of Culebra wells instrumented with downhole pressure transducers is given in Figure HYDRO-6. This figure shows the periods of time from January 2003 to the present during which pressure transducers were installed in Culebra wells. The continuous fluid-pressure measurements made using pressure transducers provide a clearer, more complete record of the changes in hydraulic head occurring in the wells than is provided by monthly water-level measurements alone. Currently, 38 Culebra wells are monitored with downhole pressure transducers. Of the wells that were monitored at one time, 3 wells shifted monitoring to a replacement well upon re-drilling (AEC-7, H-12, and H10c).

Groundwater density calculations are carried out under Activity/Project Specific Procedure SP 9-11, *Calculation of Densities for Groundwater in WIPP Wells* ([Johnson 2015b](#)). Pressure transducers are installed at mid-formation, which allows the combination of observed pressure, installation depth, and water level elevation measurements to yield an estimate of fluid density. Culebra groundwater density varies from nearly fresh in the southeastern arm of Nash Draw (e.g., H-7b1), to nearly saturated with respect to halite in wells SNL-6 and SNL-15. This procedure has been applied to both current years and historical data to produce estimates of fluid densities in wells from 2012 through 2016 ([Johnson 2013](#), [2014](#), [2015a](#), [2016](#), and [2017](#)). This approach was also used to compute 2007 Culebra groundwater densities to estimate freshwater heads required for the calibration of the Culebra groundwater flow model for CRA-2009 Performance Assessment Baseline Calculation ([Johnson 2008](#) and [2009](#)).

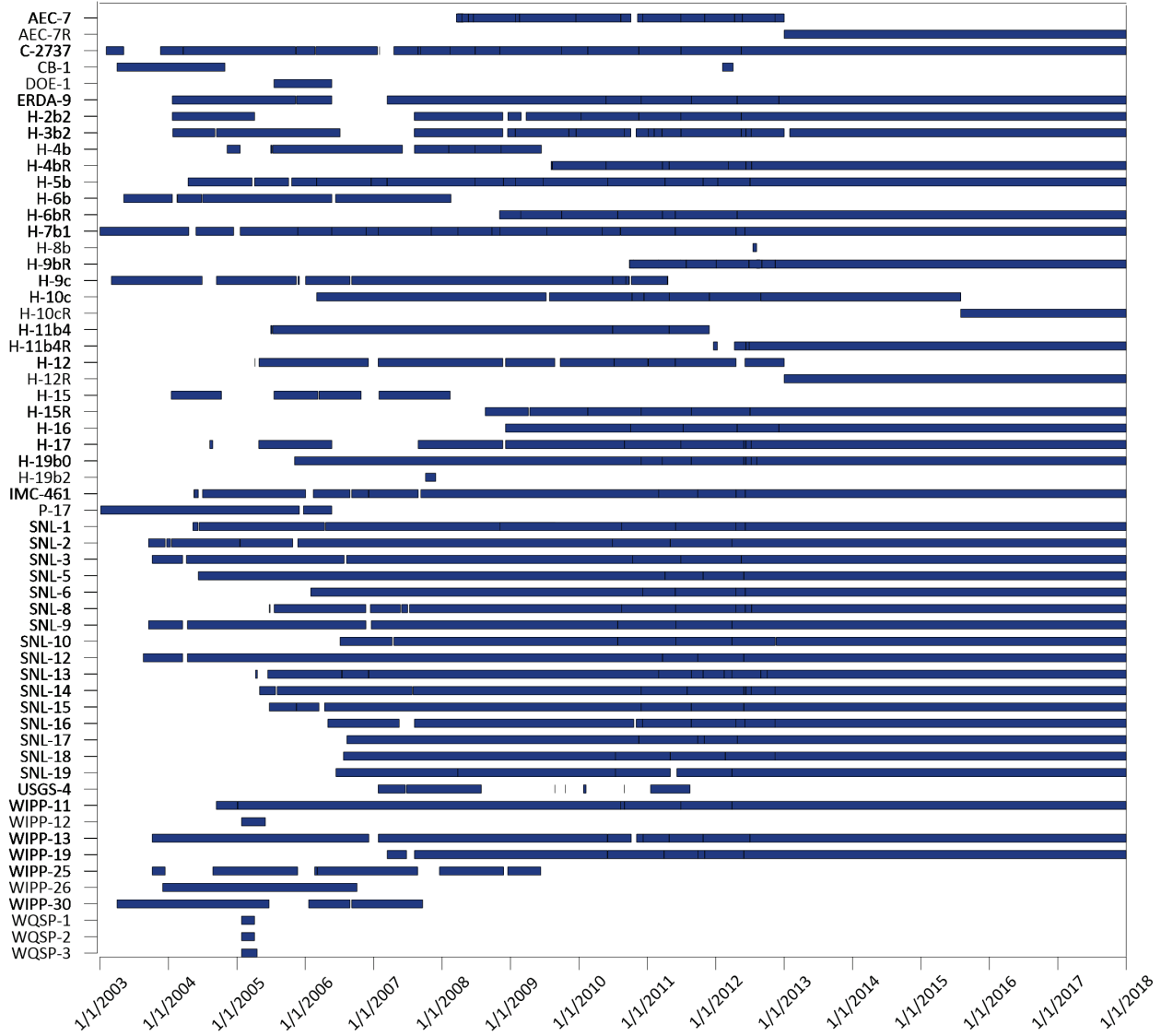


Figure HYDRO-6. Culebra Well Downhole Pressure Transducer Data Coverage

Figure HYDRO-7 through Figure HYDRO-14 show depth-to-water measurements from almost all Culebra wells monitored by the WIPP for the period from 2010 or 2012 through 2017. Refer to Figure HYDRO-1 for well locations. Wells are grouped together roughly by geographic locality, including consideration to keep together wells with similar temporal behavior or water level elevations. The reporting period for Culebra wells in this subsection was chosen to start in 2010 or 2012 (rather than 2013) to clearly show water level responses to recent events in the context of past trends.

Figure HYDRO-7, Figure HYDRO-8 and Figure HYDRO-9 show water levels from wells north of the WIPP site and in the northern portion of the WIPP site. Previously, water level trends from the majority of these wells generally paralleled one another. Starting in 2013, wells in the north central portion of the WIPP site (Figure HYDRO-9) began exhibiting a different trend from the

other north wells. The new trend is a result of new commercial activities affecting the Culebra which is discussed in Section HYDRO-6.1.2.

Figure HYDRO-7 shows water levels from wells north of the WIPP site that generally respond together. The responses correspond to seasonal rainfall events and may also capture longer drought cycles. Monthly precipitation data for the Carlsbad Airport from 2010 through 2017 is presented with the water level data in Figure HYDRO-7 (National Oceanic and Atmospheric Administration National Climate Data Center <http://www.ncdc.noaa.gov/cdo-web/>). A water level rise in 2010 was followed by general decline until the end of 2014, when water levels rose, but did not return to previously observed peak levels and have generally leveled off. Responses observed in SNL-2, SNL-18, and SNL-19 (located on the eastern edge of Nash Draw) appear to precede those in other wells, in which responses tend to be delayed. This supports the current view that precipitation effects in the Culebra progress laterally through the formation, not vertically through overlying strata.

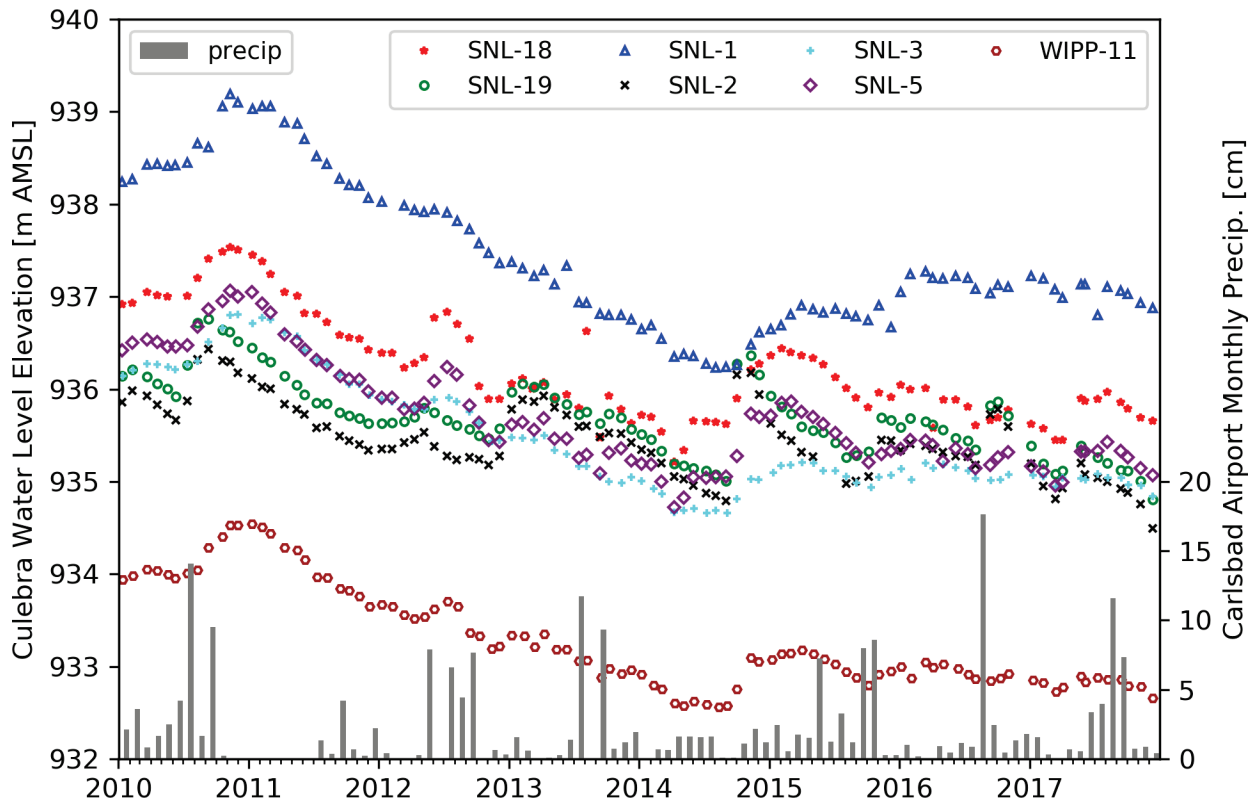


Figure HYDRO-7. Water Levels in 7 Culebra Wells North of the WIPP Site

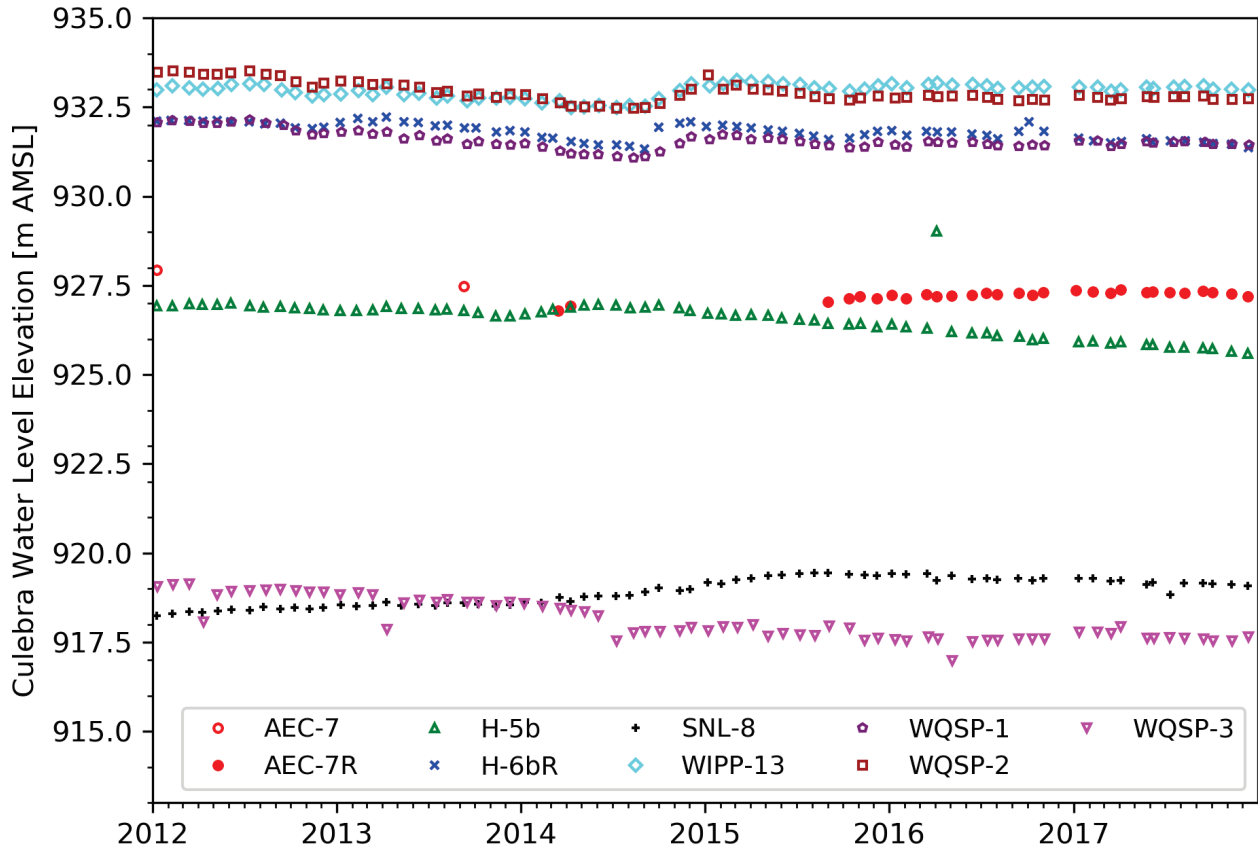


Figure HYDRO-8. Water levels in 8 Culebra Wells in the North Portion of the WIPP Site

The water level elevations plotted in Figure HYDRO-8 show similar, but more subdued trends to those in Figure HYDRO-7. Wells H-5b, and WQSP-3 do not have the same fluctuations as Culebra wells to their west and north. Annual sampling events in well WQSP-3 can be seen as drops in the water level data for that well. Gaps in the data for well AEC-7 are due to plugging and abandoning the well, development, and testing of the replacement well AEC-7R. Figure HYDRO-8 shows a filled symbol for the replacement well and an open symbol for the historic well.

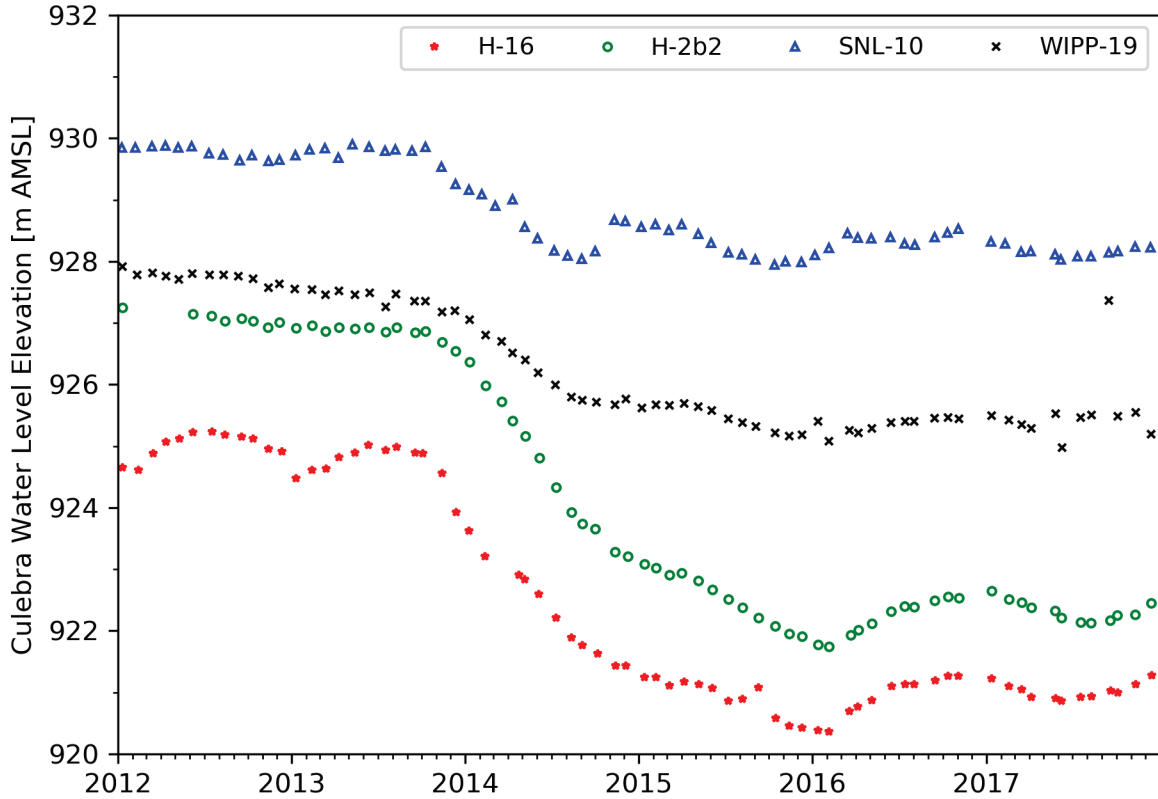


Figure HYDRO-9. Water Levels in 4 Culebra Wells in the North Central Portion of the WIPP Site

Water level elevations plotted in Figure HYDRO-9 decreased beginning in 2013 through 2016. Individual wells saw a total decrease of approximately 2 m to 5 m during this period. The drawdown is related to commercial pumping activities that began September 2013. Well WIPP-19 is the northern most wells affected by the new activity. Beginning in 2016, water levels in these wells began to stabilize or recover before dropping slightly again at the beginning of 2017. Water levels began to increase again for the remainder of 2017, likely due to slowed commercial pumping activities which are discussed further in Section HYDRO-6.1.2. Well H-16 is located within 15 m of the air intake shaft, and has historically had annual fluctuations which are believed to be related to the shaft. These fluctuations, characterized by water level drops in the winter months, were muted by the new pumping activity in both the depth-to-water measurements and continuous pressure measurements.

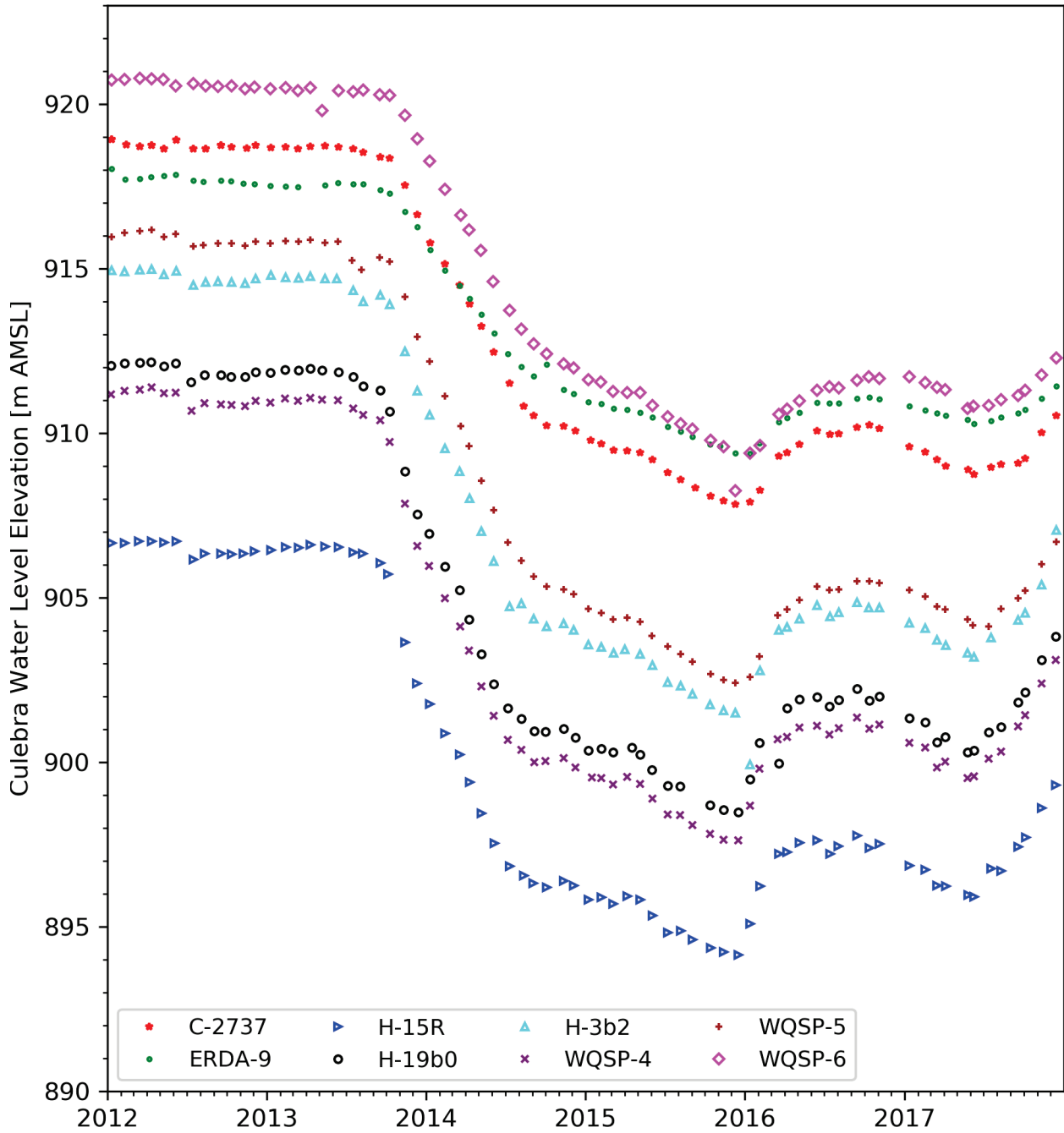


Figure HYDRO-10. Water Levels in 8 Culebra Wells in the Central Portion of the WIPP Site

Figure HYDRO-10 shows water levels from 8 Culebra wells in the central portion of the WIPP site. The water level trends in these wells mostly parallel one another, and show a stronger response to the commercial pumping affecting the Culebra aquifer than wells in the north central portion of the WIPP site (Figure HYDRO-9). Water levels in these wells dropped approximately 12 m between 2013 and the end of 2016. Water levels began to increase during 2016 before decreasing again late 2016. Water levels then began recovering mid-2017 through December 31, 2017. Previously to the new pumping event, wells in the central portion of the WIPP site had

smaller water fluctuations than northern wells (DOE 2014b). Any response to annual sampling events in the WIPP WQSP wells is muted in water level and pressure transducer data after the new commercial pumping events.

Figure HYDRO-11 shows water levels in wells located south and southeast of the WIPP site. Wells in this area were highly affected by the new commercial pumping starting in September 2013. Water level measurements in H-4bR and to a lesser extent SNL-14 and H-11bR show short term pumping cycles as well as the overall decrease in Culebra water levels in the area. Well H-4bR experienced approximately 25 m of drawdown between 2013 and 2014. The development and pumping test for replacement well H-12R accounts for the gap in water level data followed by the water level drop and partial recovery. The 2014 to 2015 data gap for well H-10c is a result of plugging and replacing with well H-10cR. The 2015 to 2016 data gap for H-10cR is related to multiple well development activities. Replacement of wells H-12 and H-10c is shown in Figure HYDRO-11 as open symbols for H-12 and H-10c and solid symbols for H-12R and H-10cR.

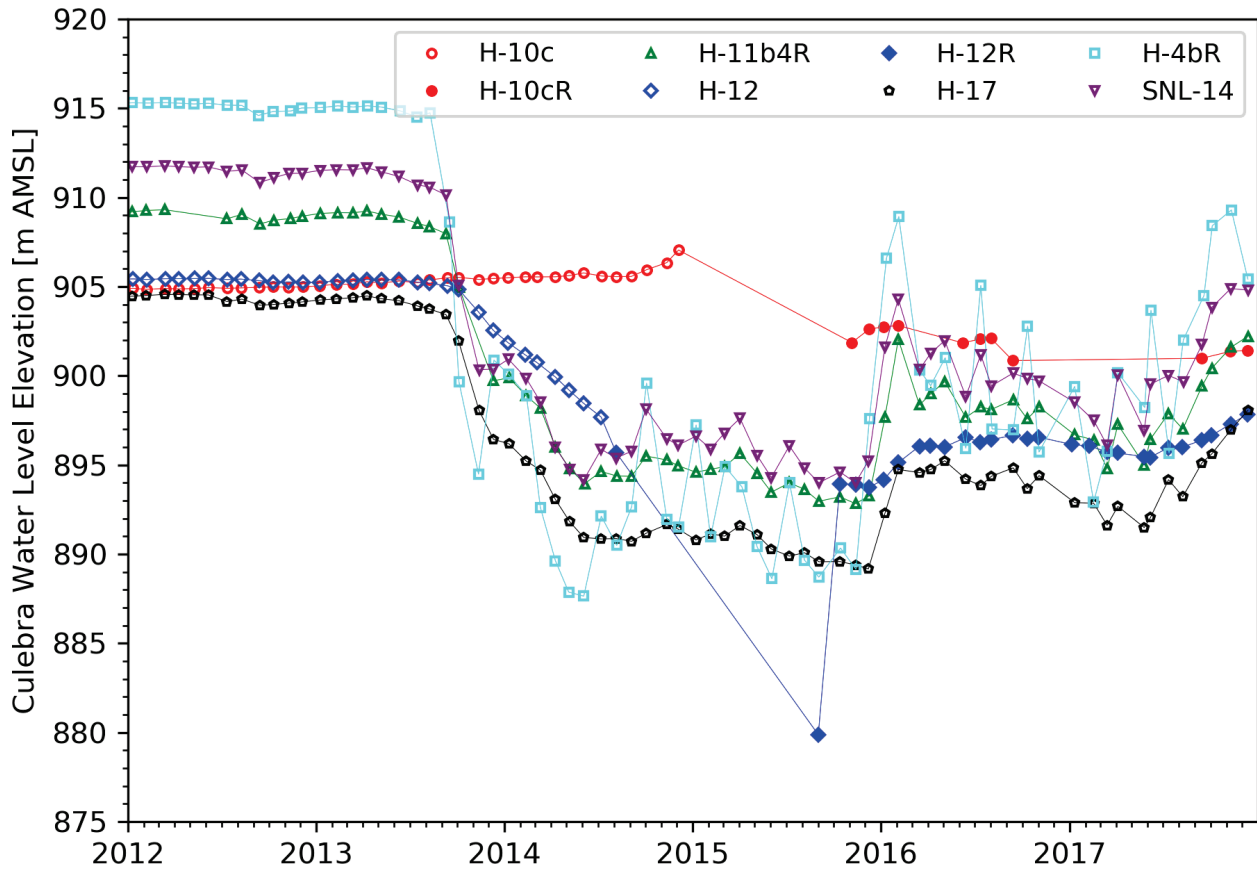


Figure HYDRO-11. Water Levels in 8 Culebra Wells South of the WIPP Site

Figure HYDRO-12 shows water level time series in wells south and southwest of the WIPP site, near the southeastern arm of Nash Draw. The Culebra produces fresher water in these areas, which is sometimes used for livestock watering and more recently the area where the new commercial pumping operation is located. The majority of the wells in this area responded to pumping by the new commercial well. Wells H-9bR, SNL-12, and SNL-17 show short term pumping cycles as well as the overall decrease in Culebra water levels in the area. Well SNL-12

experienced approximately 20 m of drawdown between 2013 and 2016. Well SNL-13 had a weaker response than other wells close to the commercial pumping well and was more similar to the response seen at the Culebra wells located in the central portion of the WIPP site.

Wells H-7b1 and SNL-16 were not affected by the pumping well (Figure HYDRO-12). These wells respond to other phenomena. A private well on the same well pad as well H-7b1 pumps for livestock watering and the well is affected by precipitation events ([Kuhlman and Corbet 2017](#)). Well SNL-16 is located within Nash Draw and responds to precipitation events such as the rain events in autumn 2014 and 2016 (Figure HYDRO-7). The responses to precipitation events are similar to events seen in Culebra wells north of the WIPP site. The 2015 gap in measurements for SNL-16 was caused by age dating experiment activities discussed in Section HYDRO-2.0.

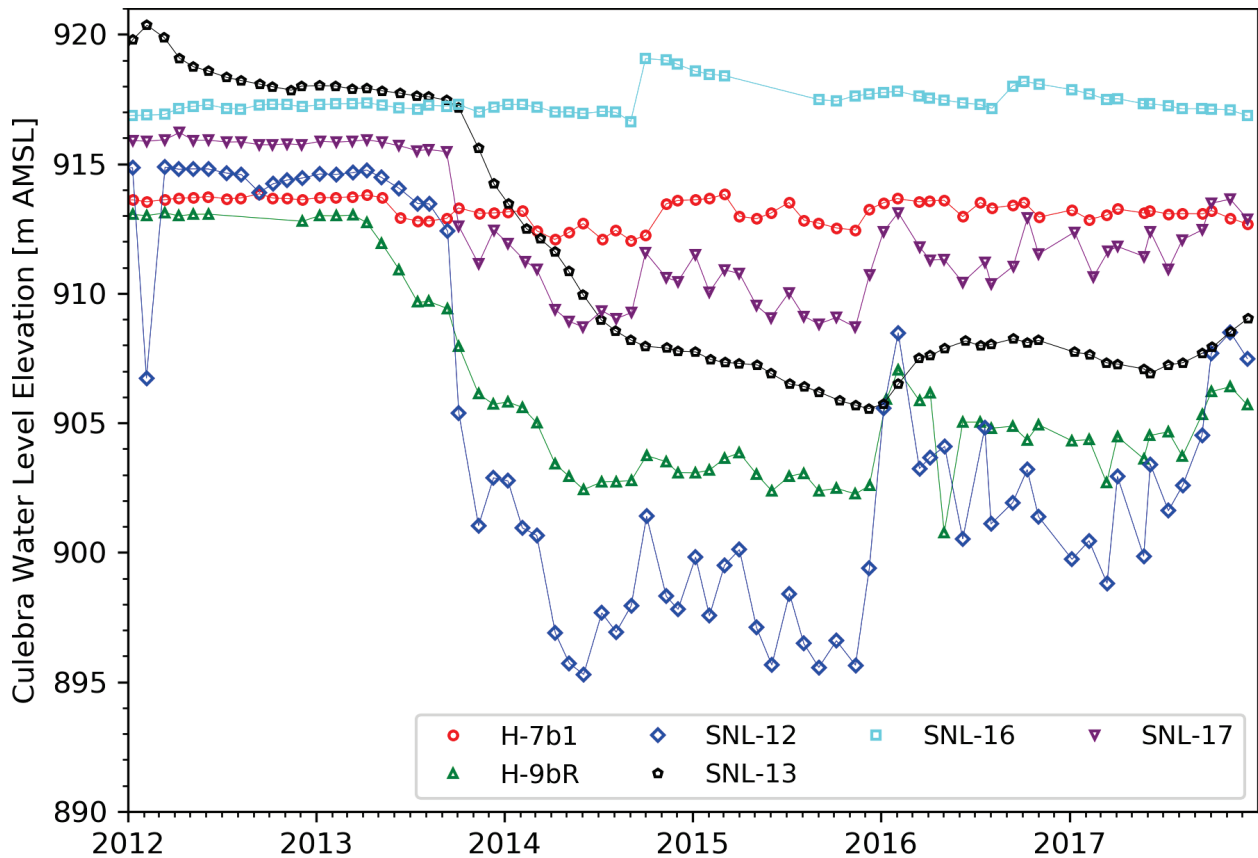


Figure HYDRO-12. Water Levels in 6 Culebra Wells in and Near the Southeastern Arm of Nash Draw

Figure HYDRO-13 shows water level time series from Culebra wells SNL-9 and IMC-461 west of the WIPP site. Data is included from 2010 through 2017 to clearly show the IMC-461 water level response to the March 2012 potash mine collapse detailed in CRA-2014 ([DOE 2014b](#)). The major upturns in water levels represent delayed responses to major rainfall events. Water levels have generally been declining.

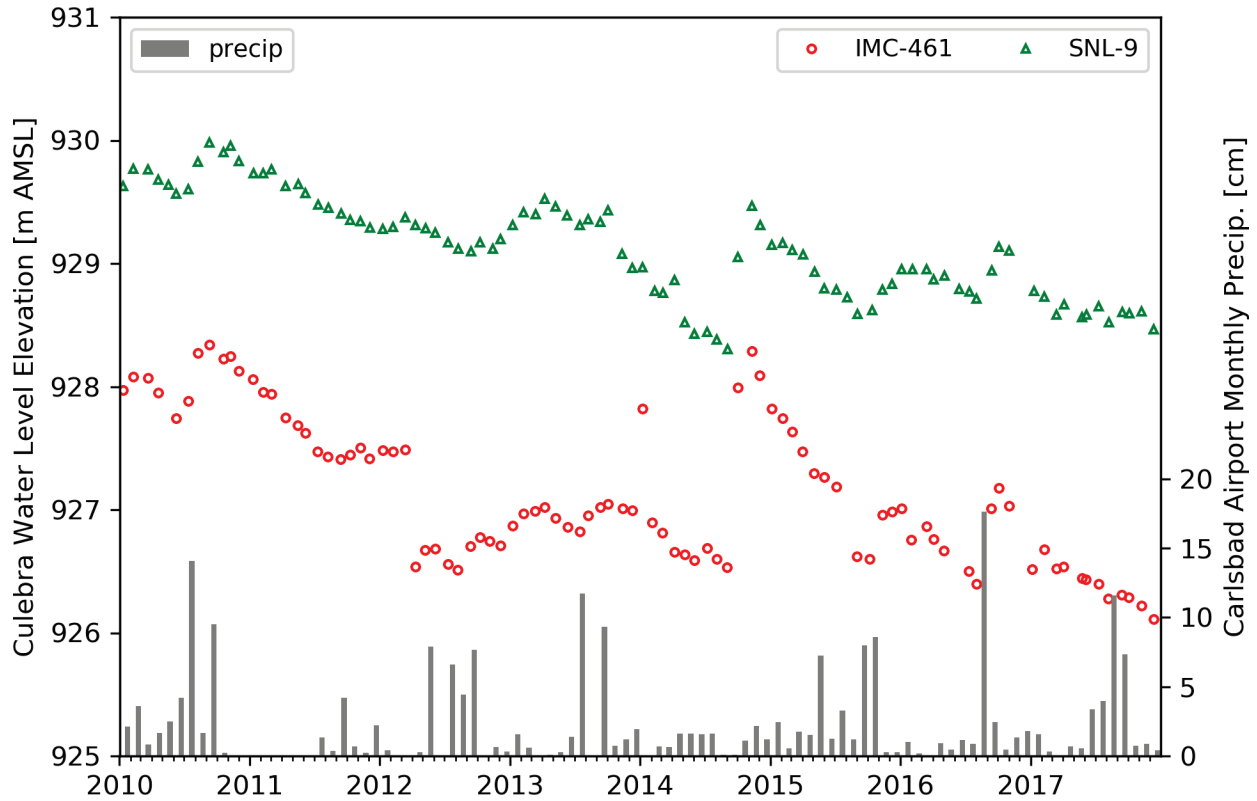


Figure HYDRO-13. Water Levels in Culebra Wells IMC-461 and SNL-9 West of the WIPP Site

Figure HYDRO-14 shows water levels from Culebra wells SNL-6 and SNL-15. These wells were drilled in areas where the Culebra contains halite cements, and are recovering very slowly from well-development activities that occurred before the plotted period ([DOE 2014b](#)). Even at the rates these wells are recovering from minor pumping and sampling (e.g., an approximately 52 m rise in SNL-6 over 6 years), water levels will not be representative of undisturbed Culebra conditions for many years.

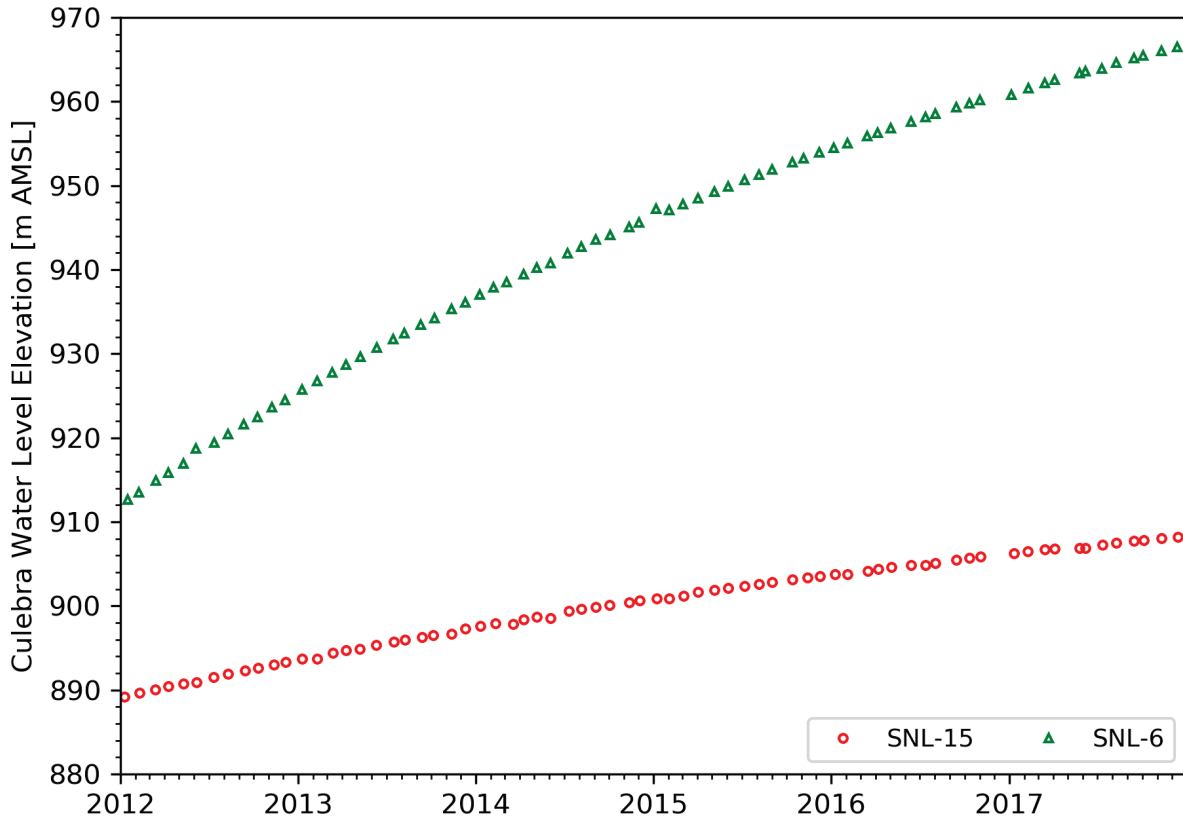


Figure HYDRO-14. Water Levels in Culebra Wells SNL-6 and SNL-15 East of the H2/M2 Halite Margin

HYDRO-6.1.2 Commercial Well Pumping

The primary event that has impacted Culebra water levels and pressures is pumping at a privately owned well, located southwest of the Land Withdrawal Boundary (LWB). Pumping began in September 2013 and continued until mid-January 2017. As mentioned in the previous section, water levels in many Culebra wells were impacted by these pumping activities. Pumping activities may be associated with the demand for local sources of water for the hydrocarbon industry in the Permian Basin. Pumping at the private well was reduced during 2017 as seen in the monthly water level measurements from Section HYDRO-6.1.1, most likely due to less demand for water by the hydrocarbon industry, and the Culebra wells in the monitoring network began to recover.

Figure HYDRO-15 shows the observed drawdown (in feet of fresh water) and partial recovery calculated from pressure transducer data at wells located at the south end of the LWB and wells further south, which are most strongly affected by pumping at the private well. Periods when the private well was likely pumping are shaded in Figure HYDRO-15. Different colors of shading indicate the three time intervals when pumping effects are evident. During the first and third pumping periods, water levels generally declined. During the second period, water levels in monitoring wells began recovering even during periods of pumping. Wells H-4bR and SNL-17 appear to respond quickest to pumping at the private well.

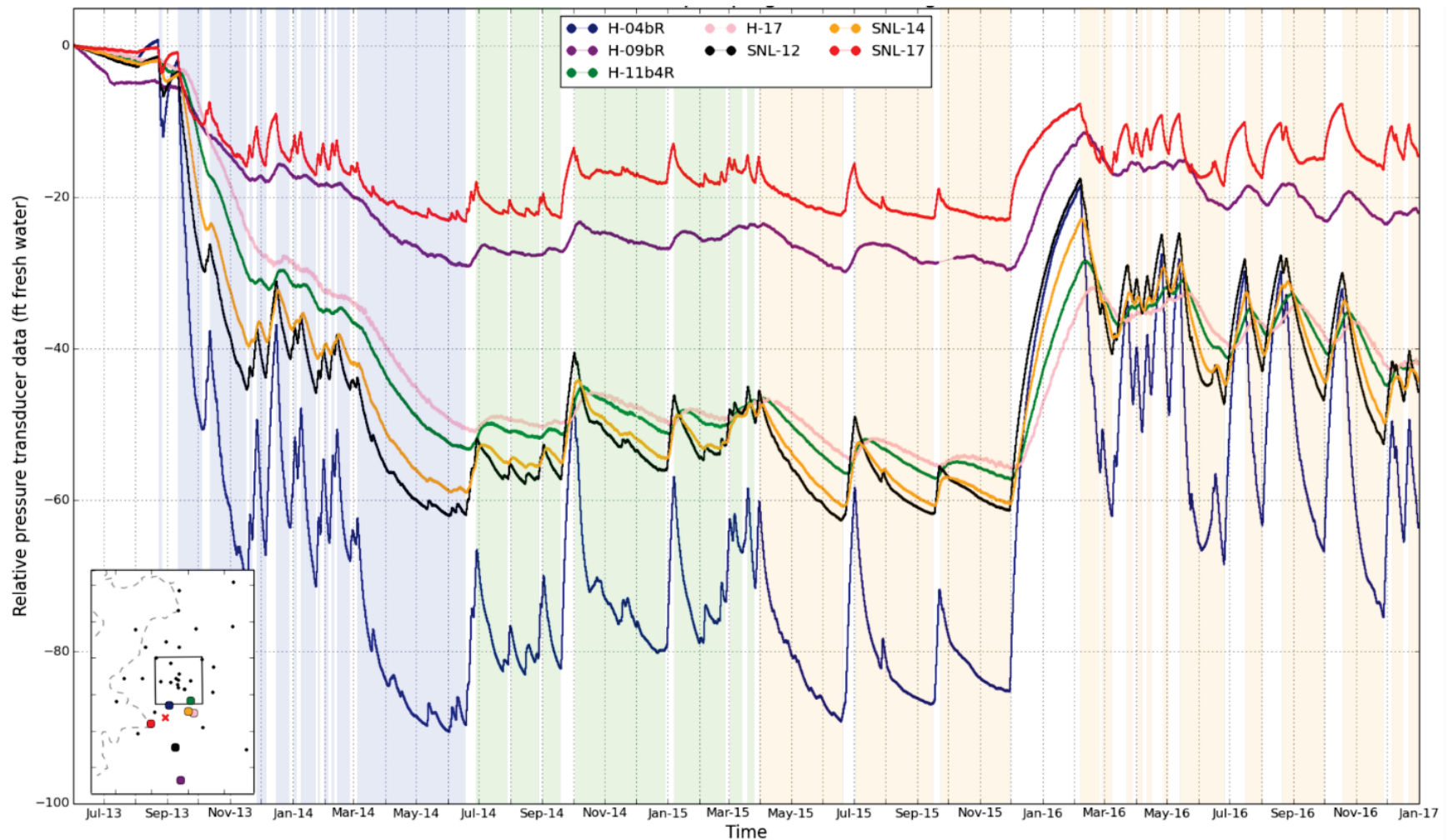


Figure HYDRO-15. Seven Culebra wells (H-4bR, H-9bR, H-11b4R, H-17, SNL-12, SNL-14, and SNL-17) responded visibly to short-term pumping cycles at a privately owned well. Likely pumping periods are shaded. The map insert at the lower left shows the location of the private well as a red “x” and the affected wells in the Culebra monitoring network are colored according to the plotted pressure transducer data lines (modified from [Kuhlman and Corbet 2017](#)).

As seen in the water level data from the previous section, wells in the central portion of the WIPP site were also affected by pumping at the private well to a lesser extent. The timing of drawdown events as well as the magnitude of the drawdown seen in these wells is consistent with expected pumping at the private well ([Kuhlman and Corbet 2017](#)). As mentioned in the water level results for wells near the southeastern arm of Nash Draw, SNL-13 responded to the private well pumping in a manner similar to the wells in the central WIPP site. Well SNL-13 is a low-transmissivity well, whereas the other wells to the southwest of the LWB tend to have high transmissivity. The low transmissivity of well SNL-13 may have contributed to the observed muted response to the pumping events, but further analysis would be necessary to verify that it is the only contributor.

Thomas et al. ([2017](#)) performed a preliminary study to estimate a pumping rate for the private well and simulate drawdown based on the first nine months drawdown was observed in the Culebra monitoring network (September 2013 through June 2014). An ensemble-averaged model from 101 spatially varying transmissivity fields was used to estimate an average pumping rate of 30.1 gallons per minute (gpm), but best-fit pumping rates for the average model range of realizations ranged between 7.0 gpm to 98.3 gpm. The attempt at simulating the observed drawdown resulted in only intermediate agreement between modeled drawdown and observed drawdown because the model used for this initial study was not modified for the high stresses imposed by a pumping well. Further development of the model would be necessary to more accurately simulate the drawdown.

HYDRO-6.2 Magenta Monitoring

Magenta water levels were monitored in 13 wells during some or all of the period 2012 through 2017 (see Figure HYDRO-1 for locations). The wells being monitored through 2017 are shown in Figure HYDRO-16 through Figure HYDRO-18. Overall, water levels in Magenta Wells were not disrupted by sampling, purging events, or hydraulic testing in the plotted 2012 through 2017 period. Small spikes in the data are caused by displacement of water during removal or replacement of instruments in the wells (e.g., well H-9c). Unlike the Culebra wells, Magenta wells do not respond to pumping at the private well. Water levels in the Magenta do not show responses to major rainfall events, thus precipitation effects seen in the Culebra come from a lateral source (where the Culebra outcrops in Nash Draw), not from vertical recharge closer to the WIPP site. These points support the assertion that there is no natural communication between the Magenta and the Culebra.

Figure HYDRO-16 shows water levels from five Magenta wells, which indicate reasonably stable water levels, aside from recovery associated with pumping and purging events before 2012. Wells H-14 and H-18 show modest, gradual increases in water level elevation over the 2012 through 2017 period, which may be due to slow recovery. Well H-2b1 is recovering from a 2010 through 2011 pumping event.

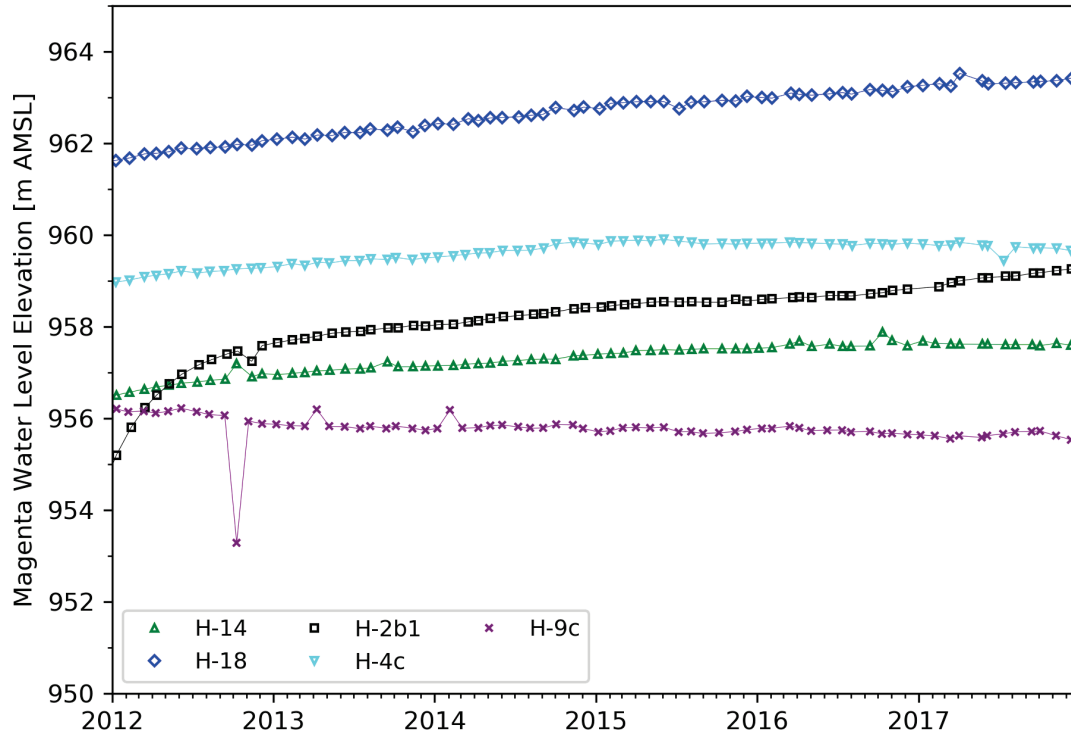


Figure HYDRO-16. Water Levels in 5 Magenta Wells

Figure HYDRO-17 shows water levels in Magenta wells that experienced large-scale fluctuations. Previously, well H-15 had been increasing steadily until early 2015, when the water level began to rise rapidly, peaking in 2016, and have been slowly decreasing. A similar, delayed water level increase was seen in the other Magenta wells (C-2737, H-3b1, H-11b2, and WIPP-18). All five wells are located within the LWB, but Magenta wells located in the eastern portion of the LWB do not show the same behavior. Further investigation is needed to determine the cause of the Magenta water level rise in eastern and central areas of the LWB.

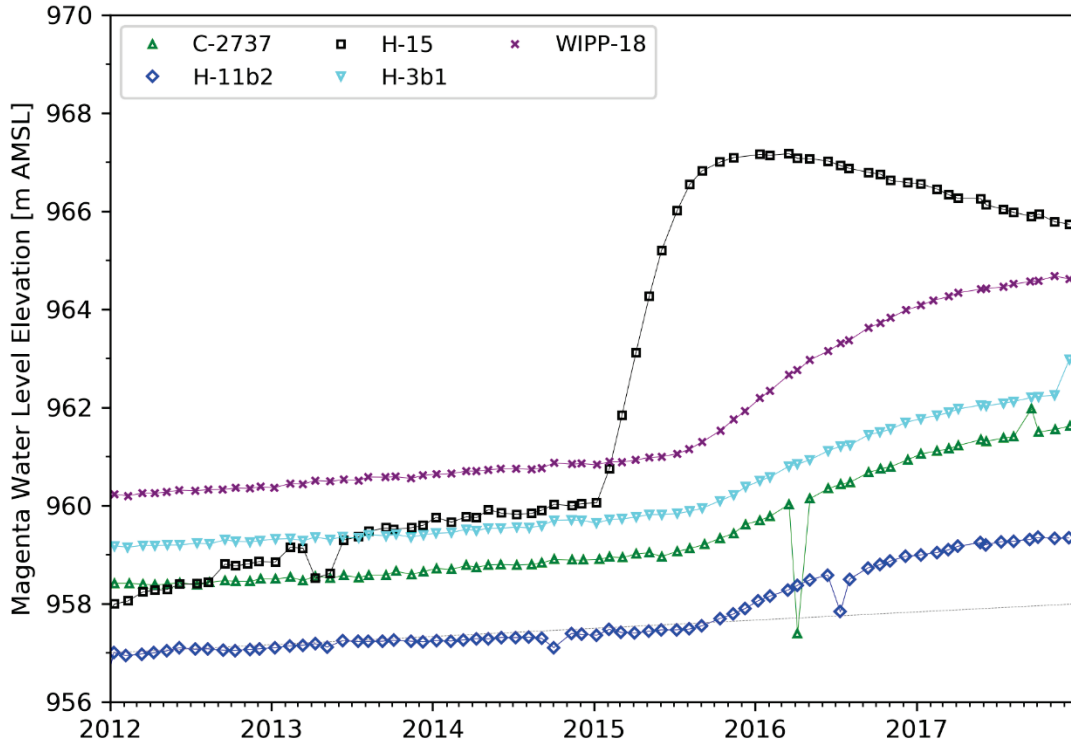


Figure HYDRO-17. Water Levels in 5 Magenta Wells

Figure HYDRO-18 shows water levels in three Magenta wells (H-10a, H-6c and H-8a). Well H-10a experienced a jump in water level during the time that Culebra well H-10cR was being drilled. Wells H-6c and H-8a have lower water levels than is typically seen in other Magenta wells. A jump in H-6c water levels in 2012 may be due to nearby oilfield activities observed at the time, although no similar response was observed at H-6bR in the Culebra. Well H-8a continued to recover from 2010 sampling activities ([DOE 2014b](#)) through 2012 and water levels have been stable since 2013.

Downhole pressure transducers are currently monitoring 13 Magenta wells (Figure HYDRO-19). The pressure transducer data are consistent with the water-level measurements made in those wells. The transducer data provide a more complete record of pumping, water-quality sampling, and other activities in the wells than the water-level data alone.

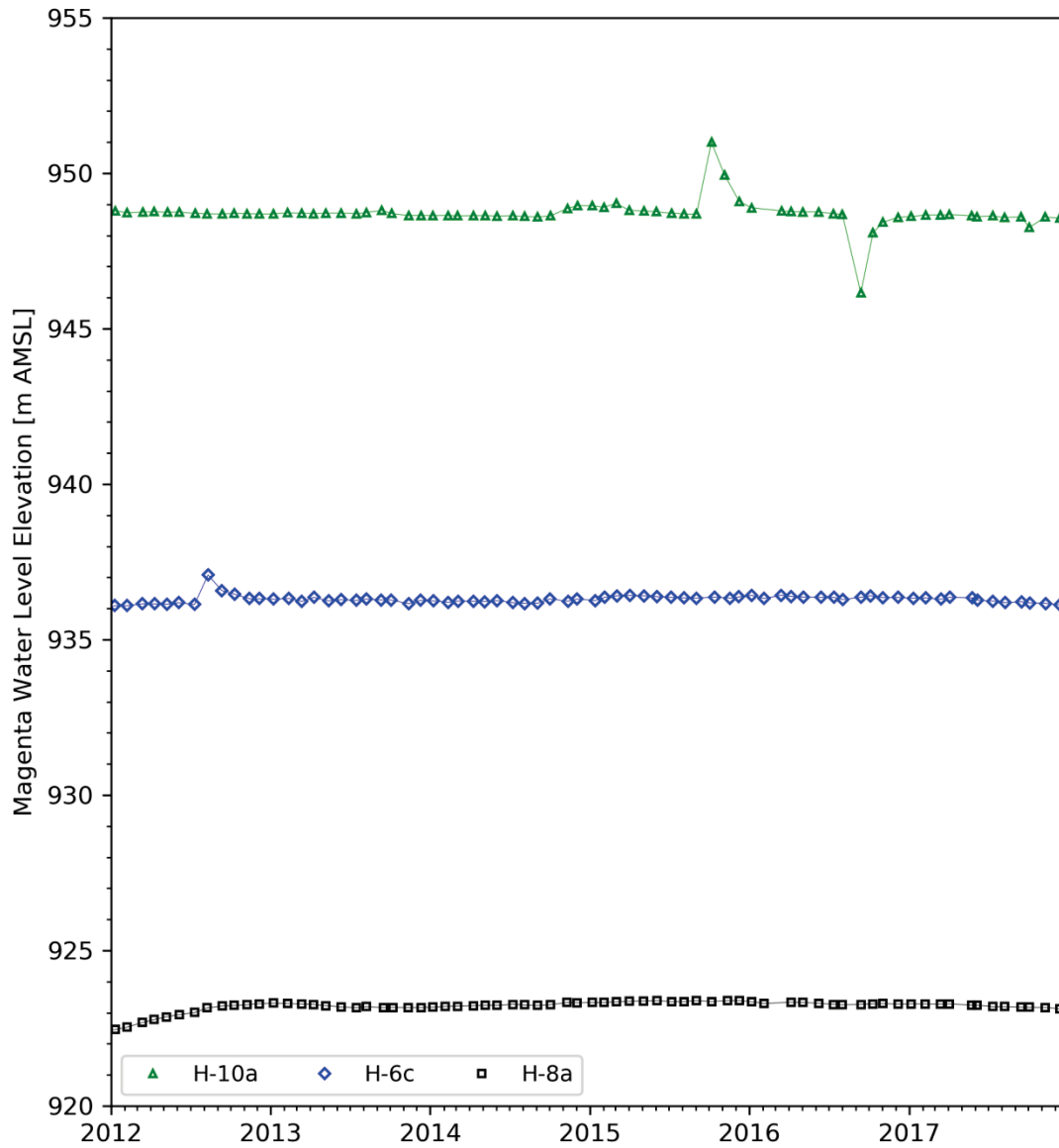


Figure HYDRO-18. Water Levels in Magenta Wells H-10a H-6c and H-8a

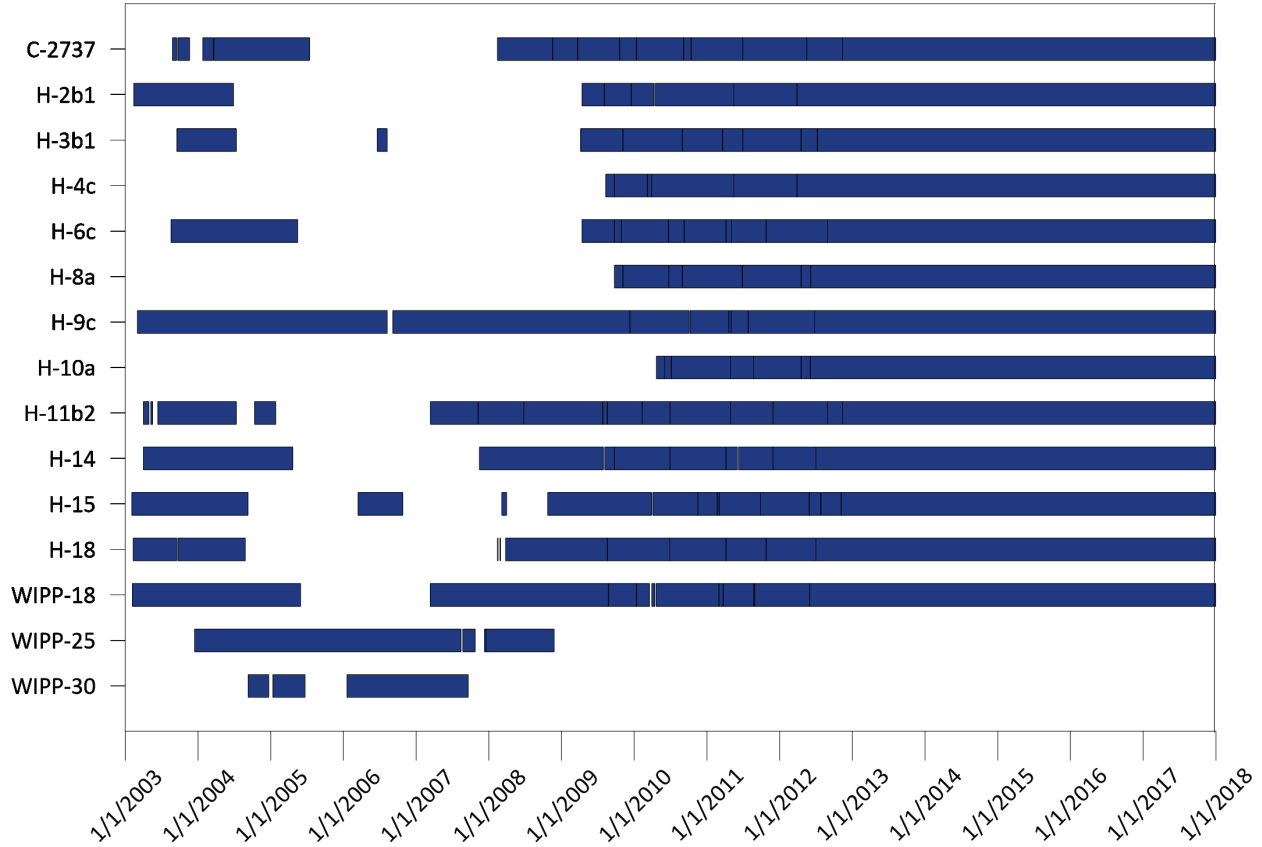


Figure HYDRO-19. Magenta Well Downhole Pressure Transducer Data Coverage

HYDRO-6.3 Dewey Lake Monitoring

The DOE monitors Dewey Lake water levels in one well, WQSP-6A. Figure HYDRO-20 shows a time series of Dewey Lake water levels in WQSP-6A from 2012 through 2017. The hydrograph shows that water levels were stable within an approximately 50 centimeters (cm) band over that period, with a slightly increasing downward trend until the latter half of 2016. The slight water level increase at the end of 2016 is most likely a response to rain events (see Figure HYDRO-7).

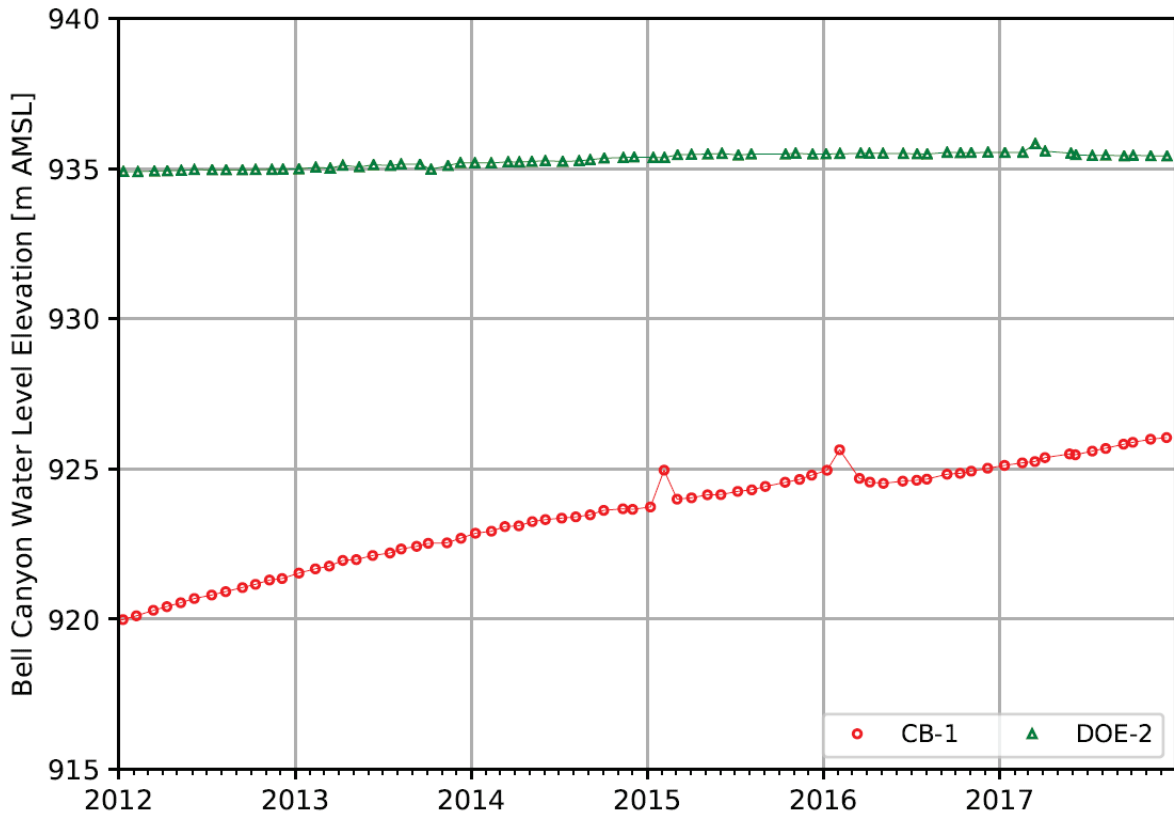


Figure HYDRO-21. Bell Canyon Water Levels

HYDRO-6.5 Monitoring Summary

Water-level monitoring provides a general picture of the changes in hydraulic head occurring in the formations being monitored. Water levels are currently being monitored in the Culebra, Magenta, Dewey Lake, and Bell Canyon. Culebra water fluctuations are generally caused by either precipitation events propagating laterally from Nash Draw or pumping from a private well south of the WIPP site. Pumping from the private well affected Culebra wells from the north central portion of the WIPP site to wells located south of the LWB. Water levels in the Magenta did not respond to pumping at the private well. Five wells in the Magenta did experience a rapid rise in water level that is not yet understood. Water levels in the other Magenta wells are generally stable or recovering from earlier pumping tests. The Dewey Lake water level (measured only in well WQSP-6A) was stable within a ~50 cm band over the last 5-year period. Bell Canyon water levels were stable in DOE-2 and rose steadily in CB-1 since being bailed in 2008.

In addition to monitoring water levels, fluid pressures in most Culebra, Magenta, and Bell Canyon wells are monitored on an hourly basis using downhole pressure transducers. The high-frequency fluid-pressure measurements provide a clearer, more complete record of the changes in hydraulic head occurring in the wells than that provided by monthly water-level measurements alone. The high-frequency pressure transducer data shows detailed fluctuations due to both

natural (barometric, earth tides, and precipitation) and man-made (potash mine collapse and oil well drilling) stimuli.

HYDRO-7.0 Culebra Heads Contour Map Generation

The creation of model-generated contour maps of Culebra piezometric head follows Activity/Project Specific Procedure SP 9-9 *Preparation of Culebra Potentiometric Surface Contour Maps* ([Kuhlman 2009](#)). Using an averaged form of the groundwater model discussed in CRA-2014 Appendix TFIELD ([DOE 2014b](#)), boundary conditions of the model are adjusted to better match each year's observed equivalent freshwater heads (the equivalent height of freshwater in a well, which equals the pressure exerted by the actual column of brine). Culebra contour maps have been generated for inclusion in the WIPP ASERs ([U.S. DOE 2013](#), [2014a](#), [2015](#), [2016b](#), and [2017](#)) annually using this procedure since 2009 ([Kuhlman 2013](#), [2014b](#), [2015](#), and [2017](#) and [Thomas 2016](#)). Figure HYDRO-22 is an example of a Culebra piezometric head contour map using data from 2013.

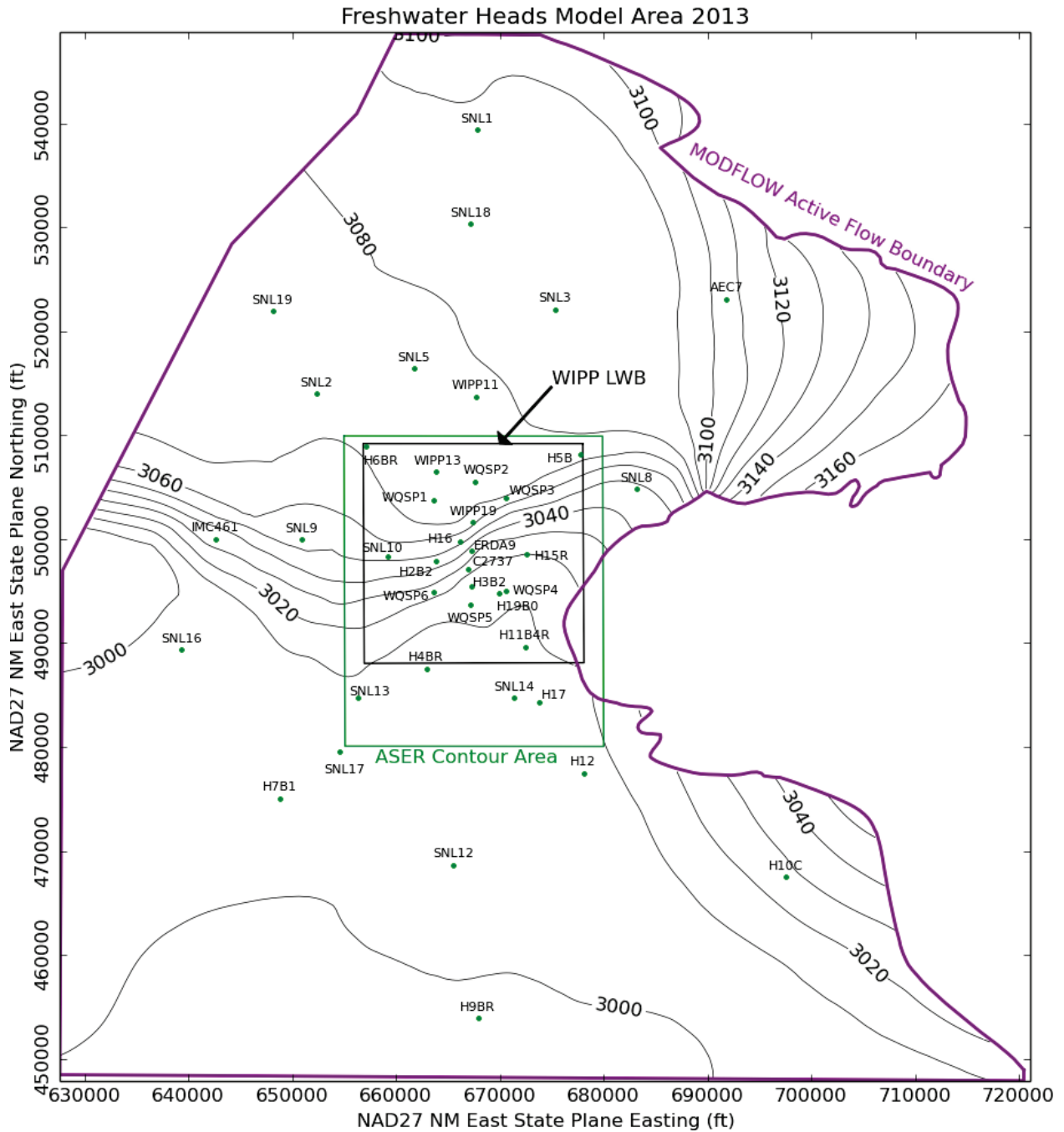


Figure HYDRO-22. Model-generated February 2013 freshwater head contours (10-foot contour interval) in the PA model domain. The green box indicates the area used in the WIPP ASER ([DOE 2014a](#)).

HYDRO-8.0 Summary and Conclusions

Radiokrypton analyses of groundwater were conducted to validate the Culebra aquifer flow model and to better understand solute transport at the WIPP ([Sturchio et al. 2014](#); [Sturchio 2016](#)). For the Culebra, we have sufficient information of the hydrogeology to apply the effects of diffusive exchange, adsorption, and salinity gradients to radiokrypton analyses to yield useful constraints on groundwater age and/or the effective diffusivity of the confining units surrounding the Culebra. The calculated age of the groundwater at the five wells tested ranges between <17,000 years and 79,000 years.

Several Culebra pumping tests were analyzed to interpret transmissivity parameter estimates at replacement well locations. Additionally, a suite of pneumatic hydraulic tests on well IMC-461 included sinusoidal tests, constant rate tests, and slug tests were compared to previous slug tests at the well. In the wells tested, variability of transmissivity in the Culebra varied over several orders of magnitude.

The WIPP groundwater-monitoring program has continued to augment monthly water-level measurements in wells with continuous (~hourly) fluid-pressure measurements using downhole programmable pressure gauges. Pressure transducer readings allow us to more clearly see effects of individual pumping events from the private well and precipitation events in Nash Draw. The pumping at the private well south of the LWB affected wells as far north as WIPP-19.

A combination of pressure and depth-to-water measurements are used to estimate fluid density in Culebra wells at the WIPP. These densities are then used to compute equivalent freshwater heads, which are combined with an averaged version of the WIPP performance assessment (PA) model to produce contour maps of piezometric head in the Culebra for inclusion in the WIPP ASER.

The nature of groundwater in the Rustler Formation, specifically the Culebra Member, has been studied in detail for several decades at the WIPP. This long history of research and investigation now serves as a firm basis for long-term monitoring of groundwater in all formations surrounding the WIPP. Effects of petroleum production and potash mining will be seen in the WIPP monitoring network for the foreseeable future. Maintenance of the current network, and investigation of observed anomalies helps to ensure both U. S. Environmental Protection Agency (EPA) and stakeholder confidence in the understanding of regional groundwater in relation to the WIPP.

HYDRO-9.0 References

(*Indicates a reference that has not been previously submitted)

Beauheim, R.L. 2009. Analysis Plan AP-070: Analysis Plan for Hydraulic-Test Interpretations, Revision 2. Carlsbad, NM: Sandia National Laboratories. ERMS 552209.

Bethke, C.M., and T.M. Johnson. 2008. Groundwater Age and Groundwater Age Dating. *Annu. Rev. Earth Planet Science*, vol. 36: 121-152.

Bowman, D.O. 2013. Analysis Report for AP-070 Analysis of the H-11b4R Pumping Test Conducted From 6/11/12 to 6/14/12. Carlsbad, NM Sandia National Laboratories. ERMS 560942.*

Bowman, D.O. 2015a. Analysis Report for AP-070 Analysis of the AEC-7R Pumping Test Conducted From 3/9/15 to 3/13/15. Carlsbad, NM: Sandia National Laboratories. ERMS 564693.*

Bowman, D.O. 2015b. Analysis Report for AP-070 Analysis of the H-12R Pumping Test Conducted From 4/20/15 to 4/22/15. Carlsbad, NM: Sandia National Laboratories. ERMS 564697.*

Bowman, D.O. 2016. Analysis Report for AP-070 Analysis of the IMC-461 Sinusoidal Test Conducted From 6/6/16 to 6/9/16. Carlsbad, NM: Sandia National Laboratories. ERMS 566972.*

Bowman D.O. 2017. Analysis Report for AP-070 Analysis of the H-10cR Pumping Test Conducted From 7/24/17 to 7/27/17. Carlsbad, NM: Sandia National Laboratories. ERMS 568762.*

Collon, P., W. Kutschera, and Zheng-Tian Lu. 2004. Tracing Nobel Gas Radionuclides in the Environment. Annual Review of Nuclear and Particle Science, vol. 54: 39-67.*

Johnson, P.B. 2008. Routine Calculations Report in Support of Task 6 of AP-114: 2007 Calculated Densities for Use in Deriving Equivalent Freshwater Heads of the Culebra Dolomite Member of the Rustler Formation near the WIPP Site, May 2007. Carlsbad, NM: Sandia National Laboratories. ERMS 548127.

Johnson, P.B. 2009. Routine Calculations Report in Support of Task 6 of AP-114: 2008 Calculated Densities for Use in Deriving Equivalent Freshwater Heads of the Culebra Dolomite Member of the Rustler Formation near the WIPP Site. Carlsbad, NM: Sandia National Laboratories. ERMS 550755.

Johnson, P.B. 2013. Memo to Records Center (Subject: 2012 Calculated Densities). February, 11, 2013. Carlsbad, NM: Sandia National Laboratories. ERMS 559277.*

Johnson, P.B. 2014. Memo to Records Center (Subject: 2013 Calculated Densities). February 6, 2014. Carlsbad, NM: Sandia National Laboratories. ERMS 561659.*

Johnson, P.B. 2015a. Memo to Records Center (Subject: 2014 Calculated Densities). February 17, 2015. Carlsbad, NM: Sandia National Laboratories. ERMS 563343.*

Johnson, P.B. 2015b. Activity/Project Specific Procedure SP 9-11, Calculation of Densities for Groundwater in WIPP Wells Revision 3. Carlsbad, NM: Sandia National Laboratories. ERMS 565218.*

Johnson, P.B. 2016. Memo to Records Center (Subject: 2015 Calculated Densities). February 23, 2016. Carlsbad, NM: Sandia National Laboratories. ERMS 565652.*

Johnson, P.B. 2017. Memo to Records Center (Subject: 2016 Calculated Densities). March 6, 2017. Carlsbad, NM: Sandia National Laboratories. ERMS 567889.*

Kuhlman, K.L. 2009. Activity/Project Specific Procedure SP 9-9: Preparation of Culebra Potentiometric Surface Contour Maps. Carlsbad, NM: Sandia National Laboratories. ERMS 552306.

Kuhlman, K.L. 2013. Analysis Report for Preparation of 2012 Culebra Potentiometric Surface Contour Map. Carlsbad, NM: Sandia National Laboratories. ERMS 560306.*

Kuhlman, K.L. 2014a. Test Plan TP 14-01: Test plan for Age Dating Sampling at the WIPP Site. Carlsbad, NM: Sandia National Laboratories. ERMS 561690.*

Kuhlman, K.L. 2014b. Analysis Report for Preparation of 2013 Culebra Potentiometric Surface Contour Map. Carlsbad, NM: Sandia National Laboratories. ERMS 562110.*

Kuhlman, K.L. 2015. Analysis Report for Preparation of 2014 Culebra Potentiometric Surface Contour Map. Carlsbad, NM: Sandia National Laboratories. ERMS 564811.*

Kuhlman, K.L. 2017. Analysis Report for Preparation of 2016 Culebra Potentiometric Surface Contour Map. Carlsbad, NM: Sandia National Laboratories. ERMS 568104.*

Kuhlman K.L., and T.F. Corbet. 2017. Memo to Records Center (Subject: WIPP Milestone Report: 2016 Culebra Groundwater Level Fluctuations). May 19, 2017. Carlsbad, NM: Sandia National Laboratories. ERMS 568172*

Lambert, S.J. 1987. Feasibility Study: Applicability of Geochronologic Methods Involving Radiocarbon and other nuclides to the Groundwater Hydrology of the Rustler Formation. Albuquerque, NM: Sandia National Laboratories. SAND 86-1054.*

Nuclear Waste Partnership (NWP). 2018. WIPP Groundwater Monitoring Program plan. Carlsbad, NM: Nuclear Waste Partnership. WP 02-1 Revision 15.*

Phillips, F.M. 2000. Chlorine-36 In: Cook, P.G. & Herczeg, A.L. (Eds.) Environmental Tracers in Subsurface Hydrology: 299-348.*

Plummer, L.N., and E. Busenburg. 2008. Evaluation of Selected Environmental Tracer Data in Ground Water from Seven Wells in the Vicinity of the WIPP Site, New Mexico. Carlsbad, NM: Sandia National Laboratories. ERMS 561539.*

Schuhen, M.D. 2010a. Test Plan TP 03-01: Test Plan for Testing of Wells at the WIPP Site, Revision 3. Carlsbad, NM: Sandia National Laboratories. ERMS 553985.

Schuhen, M.D. 2010b. Test Plan TP 06-01: Monitoring Water Levels in WIPP Wells, Revision 3. Carlsbad, NM: Sandia National Laboratories. ERMS 553993.

Sturchio, N.C., K.L. Kuhlman, R. Yokochi, P.C. Probst, W. Jiang, L. Zheng-Tian, P. Mueller, and Y. Guo-Min. 2014. Krypton-81 in Groundwater of the Culebra Dolomite near the Waste Isolation Pilot Plant, New Mexico. *Journal of Contaminant Hydrology*, vol. 160: 12-20.*

Sturchio, N.C. 2016. Results of Radiokrypton Analyses of Monitoring Wells AEC-7R, H-12R, and SNL-16 Near the Waste Isolation Pilot Plant, New Mexico. Carlsbad, NM: Sandia National Laboratories. ERMS 566236.*

Thomas, M.A. 2016. Analysis Report for Preparation of the 2015 Culebra Potentiometric Surface Contour Map. Carlsbad, NM: Sandia National Laboratories. ERMS 566114.*

Thomas, M.A., K.L. Kuhlman, and A.L. Ward. 2017. Anthropogenic Influences on Groundwater in the Vicinity of the Waste Isolation Pilot Plant, Southeastern New Mexico, USA. SAND 2016-9292c.*

U.S. Department of Energy (DOE). 1996. Title 40 CFR Part 191 Compliance Certification Application for the Waste Isolation Pilot Plant. Carlsbad, NM: U.S. Department of Energy. DOE/CAO-1996-2184.

U.S. Department of Energy (DOE). 2013. Waste Isolation Pilot Plant Annual Site Environmental Report for 2012. Carlsbad, NM: U.S. Department of Energy. DOE/WIPP-13-3507.*

U.S. Department of Energy (DOE). 2014a. Waste Isolation Pilot Plant Annual Site Environmental Report for 2013. Carlsbad, NM: U.S. Department of Energy. DOE/WIPP-14-3532.*

U.S. Department of Energy (DOE). 2014b. Title 40 CFR Part 191 Subparts B and C. Compliance Recertification Application for the Waste Isolation Pilot Plant. Carlsbad, NM: US Department of Energy Carlsbad Field Office. DOE/WIPP-14-3503.*

U.S. Department of Energy (DOE). 2015. Waste Isolation Pilot Plant Annual Site Environmental Report for 2014. Carlsbad, NM: U.S. Department of Energy. DOE/WIPP-15-8866.*

U.S. Department of Energy (DOE). 2016a. Basic Data Report for Drill Hole AEC-7R (C-3635). Carlsbad, NM: U.S. Department of Energy. DOE/WIPP-16-3567.*

U.S. Department of Energy (DOE). 2016b. Waste Isolation Pilot Plant Annual Site Environmental Report for 2015. Carlsbad, NM: U.S. Department of Energy. DOE/WIPP-16-3572.*

U.S. Department of Energy (DOE). 2016c. Basic Data Report for Drill Hole H-12R (C-3749 POD-1). Carlsbad, NM: U.S. Department of Energy. DOE/WIPP-16-3559.*

U.S. Department of Energy (DOE). 2017. Waste Isolation Pilot Plant Annual Site Environmental Report for 2016. Carlsbad, NM: U.S. Department of Energy. DOE/WIPP-17-3591.*

U.S. Environmental Protection Agency (EPA). 1996. 40 CFR Part 194: Criteria for the Certification and Recertification of the Waste Isolation Pilot Plant's Compliance with the 40

CFR Part 191 Disposal Regulations; Final Rule. Federal Register, vol. 61 (February 9, 1996): 5223–45.